Selected topics in theoretical biophysics

N. Theodorakopoulos

Konstanz, July 2001

Contents

Chapter 1

Protein structure

1.1 Introduction: the primary structure

This very brief description of protein structure will necessarily be somewhat idiosyncratic (a theoretical physicist's view).

Proteins are aperiodic biological macromolecules. Their level of structural complexity is not necessarily higher than that of a polymer. There is no branching, no polydispersity. Composition is exact.

Fundamental property of a protein: the ability to assume a soluble, compact state in water. This is accomplished by a hierarchy of interactions and structures whose net effect is to stabilize - among an astronomic number of possible alternatives - the *native conformation*. The relationship between 3-dimensional structure and function (ubiquitous in biochemistry) is defined in terms of the native conformation.

In terms of their function (or 3d structure) proteins are divided in three broad classes:

- *fibrous* (structural) proteins

- *membrane* proteins

- *globular* (enzyme) proteins.

Proteins are made of 20 amino acids (fundamental building blocks, Fig.)
Notation / Terminology (neutral amino-acid):

- C_α : $\alpha-$carbon, tetrahedrally coordinated

- NH_2: amino group

- R-group: side chain, different in each amino-acid

- COOH: Carboxyle

Chiral asymmetry: if $R \neq H$ chiral asymmetry leads to distinct steroisomers (known as D- and L-type respectively).

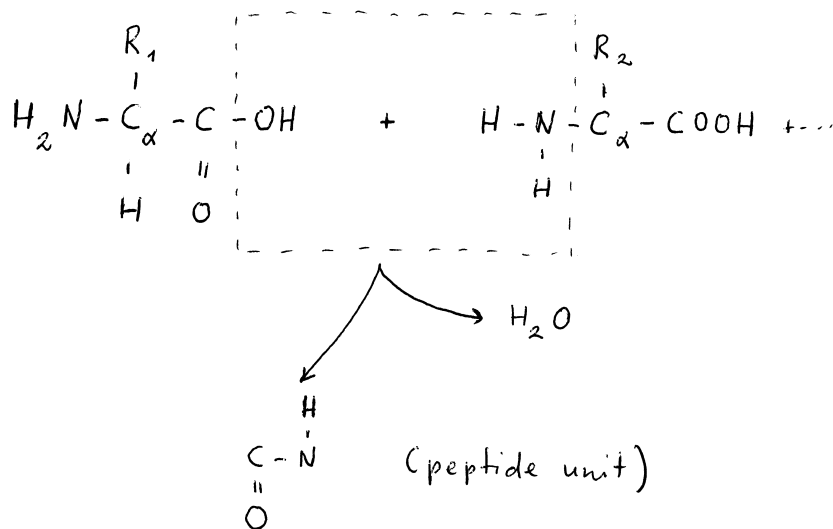   *Amino acid classification scheme* (according to R-group):

Figure 1.1: Formation of the peptide bond

1. nonpolar, aliphatic: *hydrophobic:* (from Greek $\phi o \beta o \varsigma$ = fear) [6/20].

2. polar, uncharged: *hydrophilic:* (from Greek $\phi \iota \lambda o \varsigma$ = friend) [6/20].

3. aromatic: relatively nonpolar, hydrophobic [3/20]

4. + charged (at pH 7.0) [3/20]

5. - charged (at pH 7.0) [2/20]

Building blocks put together (Fig. 1.1)

Peptide bond formation: $\Delta G = 21\ kJ/mole = 5\ kcal/mole \approx 2500K$, weak by covalent standards $(200 - 400\ kJ/mole)$, very strong by thermal standards.

More terminology:

- *peptides*: small number of amino acids linked together, usually with a defined sequence

- *polypeptides*: longer chains, but - sequence or length not strictly defined; prepared by polymerization of one or few amino acids into random sequences of varying lengths

- *proteins*: chains with a specific sequence, length and folded conformation

First level of structural organization (primary structure) $\Leftrightarrow$ sequence of amino acids)

Agent (responsible interaction): covalent bonding

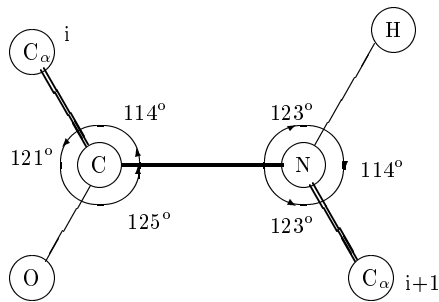at this level, the protein is simply an aperiodic 1-d chain.

3

Figure 1.2: The planar peptide group

Number of possible sequences? For a small ($N = 100$) protein there are $100^{20} \approx 10^{40}$ "possible" sequences.

Actual number of natural proteins $\mathcal{O}(10^4 - 10^5)$.

1.2 Secondary structure

X-ray expts (Astbury, 1930's) with α-*keratin* (fibrous protein, hair, wool)
findings: regular structure with a repeating unit of $5.4A$. interpretation: (Pauling & Grey, 1951)
$C - N$ bond length $1.32A$ between that of single $C - N$ ($1.45A$) and double $C = N$ ($1.22A$) bond lengths. "Partly double-bond character" As a result:
The peptide unit is planar and rigid.(Fig. 1.2)

(NB: including the neighboring C_α atoms; note that the sum of angles at both C and N equals 360 degrees.)
Rotations are possible

- around the $C_\alpha - C$ bond axis (ψ angle)

- around the $N - C_\alpha$ bond axis (ϕ angle)

Set of $\{\phi_i, \psi_i\}$ angles defines local structure (orientation of successive planar units).
Convention: $\phi = 0 = \psi$ if peptide bonds before and after a given C_α are coplanar.

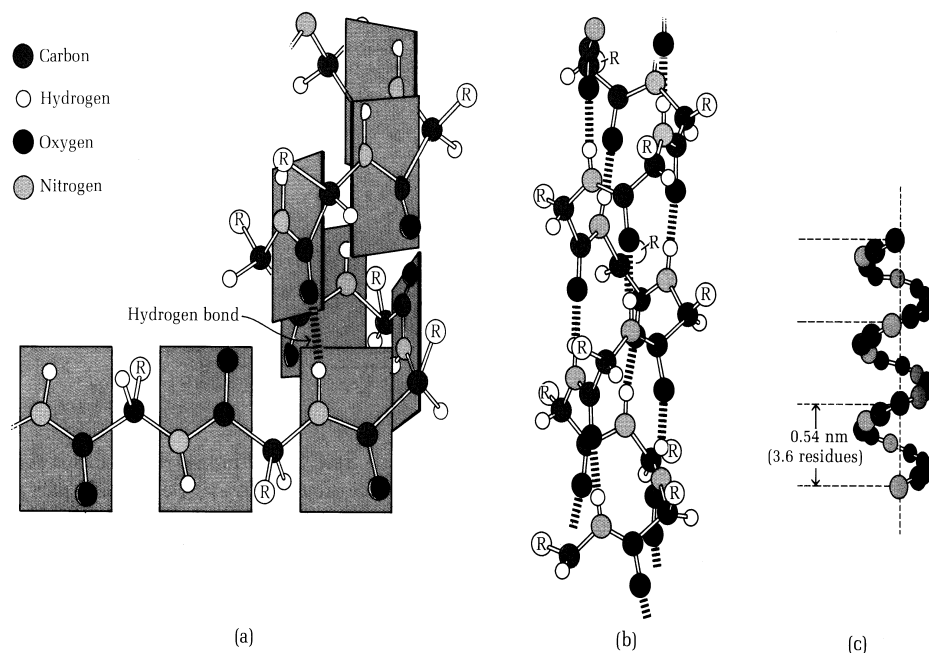$\alpha-$helical structure proposed by Pauling, has following properties:

Figure 1.3: The $\alpha-$helix in various levels of schematization. (a) shows explicitly the planar peptide units; (b) emphasizes the hydrogen bonding between N and C=O groups which are 4 residues apart in the chain; (c) shows only the backbone.

- $\phi = -57^{\circ}$, $\psi = -47^{\circ}$

- distance between monomers $p = 1.5A$ (projected along the helical axis)

- repeat distance $P = 5.4A$

- rotation angle between successive C_α atoms: 100 $^{\circ}$.

- $P/p = 3.6$ residues per turn of the helix

- exact repeat unit: $3.6 \times 5 = 18$ monomers - but

- structure is held together by hydrogen bonds connecting the N atom of the $i-$th unit to the O of the $i+4-$th unit, which is approximately above it (cf Fig)

Typical strength of H-bonds? Numbers in the literature vary from $3-6kcal/mole$ This is probably too high for the $\alpha-$helix (same magnitude as the peptide bond!) but even 1 kcal/mole should be enough to stabilize the helix. (NB: other factors may also be important in solution)

Note: what has been described is the right-handed $\alpha-$helix. A left-handed helix is in principle sterically possible. However, the side chains would come into close contact with the backbone; therefore the left-handed helix is not favored energetically.

Another common structure found in fibrous protein is the $\beta-$sheet. It also exploits hydrogen bonding for its stabilization. Dihedral angles and distances are shown in the following Table: (NB: there are other, less common, secondary structures, e.g. triple helix (collagen)).

structure	$\phi(^{\circ})$	$\psi(^{\circ})$	residues per turn	Travel per residue (A)
r-h $\alpha-$helix	-57	-47	3.6	1.5
$\beta-$parallel	-119	113	2	3.2
$\beta-$antiparallel	-139	135	2	3.4

The polypeptide chain is almost fully extended.

$\beta-$antiparallel (also in early measurements of Astbury on wool, stretched and heated)

$\alpha-$helix and $\beta-$sheets are structural elements common to "structural" proteins (collagen, $\alpha-$keratin etc.)

Systematics of dihedral angles (useful even if the overall structure is more complex, because it helps identify local structural motifs)

- *Ramachandran plots*: The method utilizes a hard sphere potential with appropriate atomic radii (can be refined to use more realistic potentials) to study what structures are sterically possible for each amino acid. The result is a "Ramachandran plot" (Fig. 1.4). It demonstrates quite nicely that $\alpha-$helixes and $\beta-$sheets fall inside the "allowed" region.
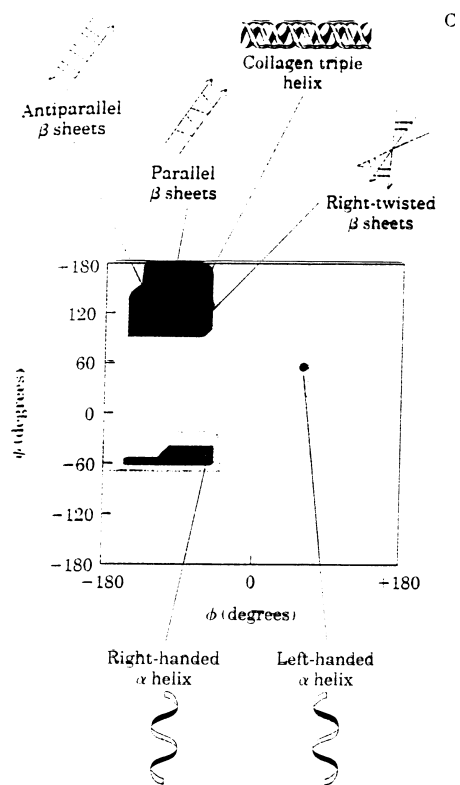
Figure 1.4: A Ramachandran plot, showing sterically allowed values of dihedral angles. Common secondary structures all fall inside allowed regions.
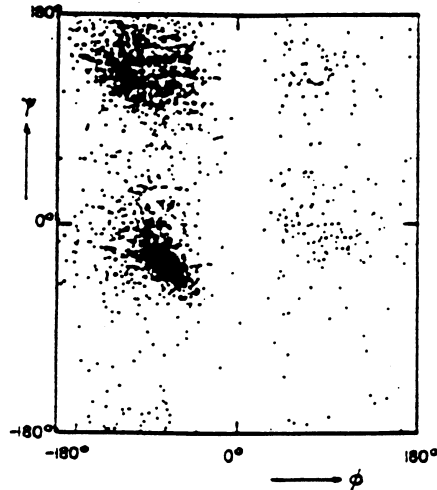
7

Figure 1.5: Statistics of dihedral angles (2500 residues 13 natural proteins, Levitt 1976)

- *statistical approach*: look at the dihedral angles of 2500 residues in 13 different proteins (Levitt, J. Mol. Biol. 1976) - Fig. 1.5 observe the concentration around both $\alpha-$helix and $\beta-$sheet characteristic values. There is significant dispersion. But the point is that such structures account for most of the local arrangement even if the exact 3-d structure is quite different in typical globular proteins.

NB: In these lectures I have made no mention of (at least) two important interactions which presumably co-determine protein structure: *electrostatic* and *van der Waals* interactions. Any complete account of protein energetics must include them!

1.3 The tertiary structure of globular proteins; folding

Key experiments: Kendrew, Perutz ca 1950
X-ray diffraction, structure of *myoglobin, hemoglobin,*
   local structure of myoglobin (153 residues) is 78% α-helical
Compact.
functional site: *heme group*
          complex organic ring structure (photoporphyrine), to which a Fe^{++} ion is bound. The ion has 6 coordination bonds, 4 in the plane of the flat porphyrine molecule and 2 perpendicular to it; one of the latter binds to a N atom, the other serves as a binding site for an O_2 molecule.
   Storage of oxygen by muscle myoglobin allows whales, seals etc. to remain
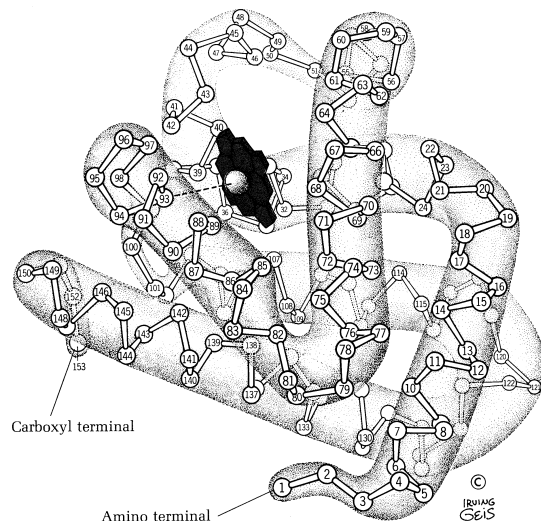
Figure 1.6: The structure of myoglobin

submerged for long periods.

The heme group must be protected from solvent, because in an oxygenated solution the ferrous Fe^{++} ion would be transformed to ferric Fe^{+++}, which does not bind O_2.

Denaturation occurs due to heat or extremes of pH.
It consists of loss of 3-d structure and function. (e.g. egg boiling: *albumin* a soluble egg protein coagulates to a white solid on heating - irreversible!)
It does *not* disrupt 1-d sequence.
Process not always irreversible.
(Option: Anfinsen expt.)
What does it disrupt? Conversely: what holds 3-d protein conformations together?
Globular proteins in solution must protect hydrophobic residues from coming into contact with water.
Key: "hydrophobic interaction" (not a Hamiltonian!).

Example: consider the solution of CH_4 in an inert, nonpolar solvent (e.g. CCl_4) compared with an aqueous solvent. (Fig) The enthalpy of solution is in both cases < 0; again, in both cases the enthalpy gain it is more than compensated by the entropy loss, which makes $\Delta G_{gas \to sol} > 0$. *Hydrophobicity is an entropic effect, and it is relative.* ΔG for an aqueous solvent is significantly higher in this example. Hydrocarbons are hydrophobic in this sense.

A direct *relative* measure of hydrophobicity for each amino acid can be given in terms of

$$Z \quad = \quad \frac{concentration\ in\ a\ nonpolar\ solvent}{concentration\ in\ water}$$

$$\Delta G \quad = \quad RT \ln Z \tag{1.1}$$

9

Amino acid hydrophobicity is correlated with accessible surface area of each side chain. (holds for hydrocarbons as well) (Fig 4.5, Creighton). Typical values of hydrophobicity: 0-3 kcal/mole.

Tertiary structure not absolutely rigid - sensitive to some "special sites".

Flexibility of the backbone allows short-range internal fluctuations - small conformational changes. Enzyme molecules must be able to undergo such changes on binding their substrates. This is part of catalytic action!
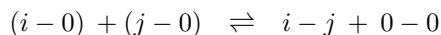
H-bonding, although important in determining local (secondary) structure, is probably present in both folded and unfolded configurations. Therefore, hydrogen-bonding interaction is not expected to dominate the formation of tertiary structure.

Statistical approach to the hydrophobic interaction

[ref: Miyazawa & Jernigan, *Macromolecules*, **18**, 534-552 (1985)]

Outline of the approach:

- visualize globular protein as a 3-d lattice, whose sites are occupied either by solvent or by an amino acid residue.

- define a "contact" between two residues as their approach within a distance of 6.5 A. Contacts due to proximity in the primary sequence do not count (covalent-determined).

- analyze a great amount of crystallographic data to determine numbers of contacts n_{ij}, n_{i0}, $(i, j = 1, 20)$, the subscript 0 stands for water.

- consider the "chemical reaction"

$$(i - 0) + (j - 0) \quad \rightleftharpoons \quad i - j + 0 - 0$$

$$\frac{n_{ij}n_{00}}{n_{i0}n_{j0}} \quad = \quad \exp\left(-\frac{e_{ij}}{RT}\right) \qquad (1.2)$$

  and assign "interaction energies" e_{ij}, by fitting to the populations n_{ij}.

- result: 20 x 20 symmetric matrix (210 independent elements).

A further step along this direction has been done by the work of Li, Tang & Wingreen, *PRL* **79**, 765 (1997). They have fitted the elements of the Miyazawa-Jernigan matrix to the form

$$e_{ij} = C_0 + C_1(q_i + q_j) + C_2 q_i q_j \qquad (1.3)$$

reducing the number of constants to 23 (The 3 C's and 20 q's, one for each amino acid; moreover, the extracted q's fall into two groups (polar and hydrophobic) and - except in the cases of charged aminoacids - correlate well with measured hydrophobicities.

The model is good starting point for a semiquantitative approach to the protein folding problem.

protein folding (the issue):

Given the 1-dimensional sequence, predict the 3-dimensional structure (*)

(highly nontrivial, yet seems to be part of the genetic program).

Consider: if each monomer can assume an average of γ (one estimate: $\gamma \approx 4.6$)) independent local conformations, a chain of N monomers has γ^N independent conformations. Even for a small protein (N=100) the number is huge. Sampling available conformational space for the "right" arrangement at the rate of 1 flip per psec is hopelessly slow. Yet (Levinthal paradox) folding is achieved in a time scale of msec to sec. "Gracious folding", efficient folding etc - On the other hand, naturally occurring proteins are a tiny fraction of all possible amino acid sequences. This raises the question of an evolutionary bias towards "good folders".

The latter issue is a strictly biological one. Physics can attempt to answer the [strictly physical question] (*), or the more qualitative:

given the 1-d sequence and the 3-d structure, describe the folding path. (**)

A Monte-Carlo simulation of protein folding
Ref: Sali, Shakhnovich & Karplus, *Nature* **248**, 364 (1994)

The model:

- Monomer beads on a cubic lattice

- chain of $N = 27$ monomers

- "Hamiltonian"
$$H = - \sum_{all\ pairs\ (ij)} \Delta_{i,j} B_{i,j} \qquad (1.4)$$

  where
$$\Delta_{i,j} = \left\{ \begin{array}{ll} 1 & \text{if } i,j \text{ in contact} \\ 0 & \text{otherwise} \end{array} \right. \qquad (1.5)$$

  and the interaction parameters are random, overall attractive (hydrophobic, consistent with Miyazawa-Jernigan)

- MC trials: shift one or two monomers at a time (cf Fig);
  accept or reject changes according to Metropolis algorithm
$$\begin{array}{ll} if\ \Delta E < 0 & \text{accept} \\ if\ \Delta E > 0 & \text{accept with probability } e^{-\beta \Delta E} \end{array} \qquad (1.6)$$

MC experiment generates 200 sequences with random interactions.
Follow

- the total energy ϵ

- the number of total contacts (native as well as non-native) N_c

- the fraction of native contacts Q_0

Findings:
Not all sequence fold to a globular state in a reasonable time (1.5×10^7 MC steps). 30 of the 200 do. MC kinetics is reasonably related to natural thermal motion of a native protein in solution.
(i) Folded conformation, (ii) summary of kinetics and (iii) energy spectra in first figure.
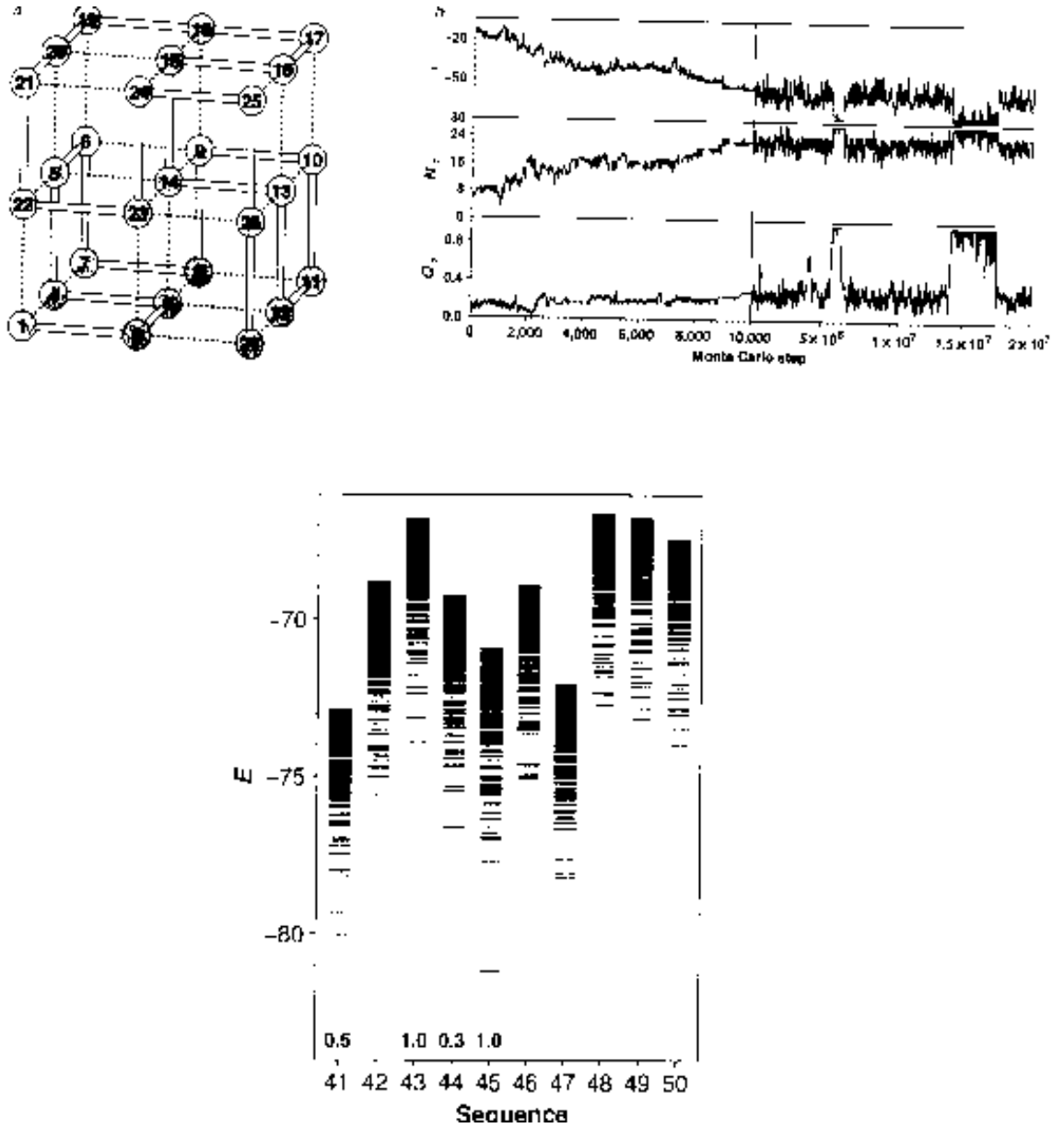
Figure 1.7: clockwise from top left: (i) the folded conformation (ii) Evolution of N_c, the number of contacts and Q_c, the fraction of native contacts; (iii, bottom) Energy levels for a number of sequences; the numbers from Ref. (). Good folders (characterized by a fraction of native contacts close to unity), are distinguished by a well separated grounded state.
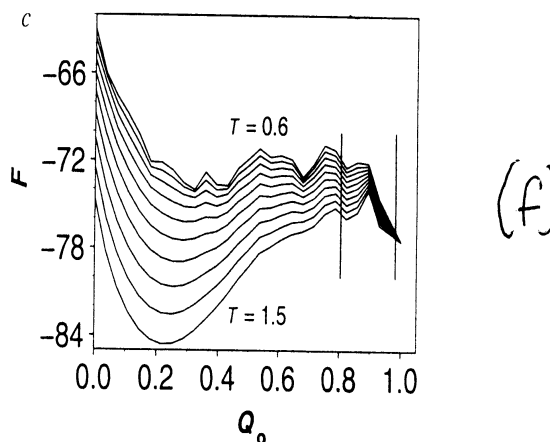
Figure 1.8: free energy vs fraction of native contacts for a range of temperatures; at low temperatures, the minimum corresponds to the folded state; note that at the lowest temperatures the curve becomes "rugged". At higher temperatures denaturation occurs (minimum at $Q_0 \approx 0.3$)

The kinetics suggest a 3-state approach to folding: the first stage is fast ($\sim 10^4$ steps, after which a semicompact structure is achieved, with $Q_0 \sim 0.3$; the second stage is slow ($10^6 - 10^7$ steps and achieves the "transition region". The final stage involve sampling of the transition region itself, and is quite rapid.

It appears that the necessary and sufficient condition for successful folding is the existence of a well separated state of minimum energy.

By "binning" together states within a given interval of total energy and native contact fraction, it is possible to obtain a two-dimensional histogram; the statistics are described by

$$\nu(Q_0, \epsilon) = \omega(Q_0, \epsilon)e^{-\beta\epsilon} \tag{1.7}$$

where the first factor is a temperature independent density of states; summing (1.7) over all energies,

$$Z(Q_0, T) = \sum_{\epsilon} \nu(Q_0, \epsilon) \tag{1.8}$$

it is possible to obtain a "partition function" and a corresponding thermodynamic free energy; the latter is shown in the Fig 1.8. The study reveals a "thermodynamic phase transition" around $T = 1.1$. At lower temperatures, the free energy minimum is at $Q_0 = 1$ (folded state); note however the "rugged" structure at very low temperatures (cf. protein glass, next chapter). At higher temperatures the system seems to favor a denatured state with a low fraction of native contacts($Q_0 \approx 0.3$).

In conclusion: the model, despite its considerable simplicity, seems to describe some of the gross features of the folding process.

Chapter 2

Collapsed & frozen polymers - Glassy proteins

2.1 Geometrical considerations, Flory theory

(Sections 1-3 adapted from Wolynes & Bryngelson, *Biopolymers*, **30**, 177 (1990)).
Chain of N monomers with nearest-neighbor distance l.
End-to-end vector $\vec{R}$.
Distribution of $R = |\vec{R}|$ according to

$$P(R)dR = \frac{C}{R_0}\left(\frac{R}{R_0}\right)^2 e^{-\frac{3}{2}\left(\frac{R}{R_0}\right)^2} dR \tag{2.1}$$

where $R_0^2 = Nl^2$ is the mean square distance which corresponds to a random walk.

Number of conformations: obtained by "coarse graining". Each monomer is estimated to have ν_0 distinct conformations. For a *lattice polymer*, this would be equal to z, the *coordination number* of the lattice. For an "ideal polymer", the number of distinct conformations with end-to-end distance in the interval $(R, R + dR)$ would therefore be

$$\Omega_i(R)dR = \nu_0^N P(R)dR \,. \tag{2.2}$$

This number is not realistic, because it does not take account of the monomers' tendency to avoid close contact with other monomers ("excluded volume effect"). This can be done in the following fashion:

Definitions:
Total volume of polymer in a given conformation:

$$V = \gamma R^3 \tag{2.3}$$

Monomer volume:

$$v_m = \gamma \sigma^3 \tag{2.4}$$

(use same value of γ by convention, i.e. choose σ accordingly.
Generalized packing fraction: ratio of volume occupied by all monomers to total volume

$$\eta(R) = \frac{Nv_m}{V} = N\left(\frac{\sigma}{R}\right)^3 \tag{2.5}$$

Now, visualize the monomer as being put together "bead by bead" wthin the volume V. Each successive monomer "sees" a higher fraction of volume occupied. Thus, the first bead is under no constraint at all, the second bead sees a fraction v_m/V of the total volume occupied, the third a fraction $2v_m/V$, the mth a fraction $(m-1)v_m/V$. We argue that the number of available conformations must be reduced by a factor *(1 - fraction of occupied volume)* at each step. This results in an overall reduction by

$$
\begin{aligned}
\omega_{E.V}(R) &= \prod_{m=1}^{N} \left(1 - (m-1)\frac{\eta(R)}{N}\right) \\
&= \left(\frac{\eta}{N}\right)^N \prod_{m=1}^{N} \left(\frac{N}{\eta} - m + 1\right) \\
&\approx \left(\frac{\eta}{N}\right)^N \left(\frac{N}{\eta}\right)\left(\frac{N}{\eta} - 1\right) \cdots \left(\frac{N}{\eta} - N + 1\right) \\
&\approx \left(\frac{\eta}{N}\right)^N \frac{(N/\eta)!}{(N/\eta - N)!} \, .
\end{aligned}
\tag{2.6}
$$

Using Stirling's approximation $\ln N! \approx N \ln(N/e)$ for large N and N/η, we further obtain

$$
\ln \omega_{E.V} = N \left(1 - \frac{1}{\eta}\right) \ln(1 - \eta) - N \, .
\tag{2.7}
$$

Combining all geometric considerations, we obtain the number of conformations for a "real" polymer

$$
\Omega_0(R)dR = \omega_{E.V} \nu_0^N P(R) dR \, .
\tag{2.8}
$$

or, in terms of the entropy

$$
\begin{aligned}
S_0 &\equiv \ln \Omega_0 \tag{2.9} \\
&= N \ln \nu_0 + N(1 - \frac{1}{\eta}) \ln(1 - \eta) - N + 2\ln(\frac{R}{R_0}) - \frac{3}{2}\left(\frac{R}{R_0}\right)^2 \tag{2.10}
\end{aligned}
$$

where we have neglected contributions which are of order N^0 or lower (e.g. normalization constants).

Exercise (unnumbered): Integrate $\Omega_0(R)$ over all R to find the total number of conformations geometrically available to the polymer

Exercise (unnumbered): Compute the average (strictly: most probable) end-to-end distance for a non-ideal polymer.

Solution: Use a low η expansion in the second and third term in the expression (2.10) for the entropy and minimize with respect to R.

$$
(1 - \frac{1}{\eta}) \ln(1 - \eta) - 1 \approx -\frac{\eta}{2} - \frac{\eta^2}{6} \, .
\tag{2.11}
$$

Keeping the leading term, and dropping the logarithmic term in (2.10), we obtain

$$
S_0(R) \approx N \ln \nu_0 - N\frac{\eta}{2} - \frac{3}{2}\left(\frac{R}{R_0}\right)^2 \, .
\tag{2.12}
$$

Minimizing $S_0(R)$ gives

$$\begin{aligned}
\frac{\partial S_0(R)}{\partial R} &= -N\frac{1}{2}\frac{\partial \eta}{\partial R} - \frac{3}{2}\cdot 2\frac{R}{R_0^2} \\
&= N\cdot\frac{1}{2}N\cdot 3\frac{\sigma^3}{R^4} - 3\frac{R}{R_0^2} ,
\end{aligned}$$

and a most probable distance

$$\begin{aligned}
\bar{R}^5 &= \frac{1}{2}N^2\sigma^3 R_0^2 \\
\bar{R} &= \left(\frac{\sigma^3}{2l^3}\right)^{1/5} N^{3/5}l \tag{2.13}
\end{aligned}$$

(Flory's 3/5 approximate law for the self-avoiding random walk; more generally in d dimensions the approximate theory described here predicts $\bar{R} \propto N^\nu$ with $\nu = 3/(d+2)$. The prediction is exact in 1 and 2 dimensions and comes remarkably close to the renormalization group result 0.5880 ± 0.0015 in 3 dimensions).

2.2 The collapse of random heteropolymers

Until now, arguments were based purely on geometrical grounds. In order to examine the effects of temperature (in solution) it is necessary to formulate a theory of polymer thermodynamics. To do this we need to know something about the *energetics* of polymers in solution. A useful concept in this context is that of a "random heteropolymer" with an overall attractive interaction between monomers which come into contact with each other. (Note: "Contact" in this sense excludes those monomers which are nearest neighbors in the chain.) The overall attraction reflects the overall hydrophobic tendency of a polymer in solution. Assume an average value $\bar{K}$ and a standard deviation ΔK for the energy of two interacting monomers. (Note: in the limit $\Delta K \to 0$ the theory describes homopolymers).

The number of contacts $I(R)$ between monomers is determined by geometry; for every monomer it is proportional to packing fraction. This gives a total number of contacts

$$I(R) = z\eta(R)N \tag{2.14}$$

where z is a geometrical factor; accordingly, the mean-field energy and its variance are given by

$$\bar{E}(R) = -\bar{K}I(R) \tag{2.15}$$

and

$$\Delta E^2(R) = (\Delta K)^2 I(R) \tag{2.16}$$

respectively. For a given polymer size, we will assume a Gaussian distribution

$$g(R,E) = \frac{1}{\sqrt{2\pi\Delta E^2(R)}}e^{-\frac{[E-\bar{E}(R)]^2}{2\Delta E^2}} . \tag{2.17}$$

of energy states around the mean field value. It is now possible to calculate the number $n(E)dE$ of polymer conformations of any size in a given energy interval

16

$(E, E+dE)$ by integrating Ω_0 over R, weighted according to the Gaussian (2.17):

$$n(E) = \int_0^\infty dR \underbrace{g(R, E)\, \Omega_0(R)}_{\equiv\, e^{S(R,E)}} > .\tag{2.18}$$

The above integral is expected to be sharply peaked at large values of N. If we are not interested in prefactors -this is the case throughout this chapter- we estimate its value by the maximum of the integrand, i.e.

$$n(E) \approx e^{S(\bar{R}, E)}\tag{2.19}$$

where

$$S(R, E) \approx \underbrace{\ln \Omega_0(R)}_{S_0(R)} - \frac{\left[E - \bar{E}(R)\right]^2}{2\Delta E^2}\tag{2.20}$$

and $\bar{R}$ is the value of R which maximizes $S(R, E)$ at given E. Accordingly, $S(\bar{R}, E)$ is the average entropy as a function of the energy.

The above, microcanonical formulation of polymer statistical mechanics, which maximizes entropy at constant energy is not well suited for applications. To describe the physics at a given *temperature* T, we introduce a Legendre transform $(\partial S/\partial E) = 1/T$ and minimize the free energy function $F = E - TS$ instead: [1]

From the definition of temperature

$$\frac{\partial S}{\partial E} = -\frac{\left[E - \bar{E}(R)\right]^2}{2\Delta E^2} = \frac{1}{T}\tag{2.21}$$

it follows that E (now, like S, a function of R and T) is given by

$$E = \bar{E}(R) - \frac{\Delta E^2(R)}{T} .\tag{2.22}$$

Introducing (2.22) in (2.20) we obtain

$$S = S_0(R) - \frac{\Delta E^2(R)}{2T^2}\tag{2.23}$$

and hence

$$F(T, R) = \bar{E}(R) - \frac{\Delta E^2(R)}{2T} - TS_0(R)\tag{2.24}$$

---

[1] A quick way to recognize the mathematical basis for this procedure is to consider the identity

$$\frac{d}{dx}S(x, E) = \left(\frac{\partial S}{\partial E}\right)_x \frac{dE}{dx} + \left(\frac{\partial S}{\partial x}\right)_E .$$

Maximization of S at constant E demands that the second term in the r.h.s. should vanish. The above identity states that, if $\left(\frac{\partial S}{\partial E}\right)_x$ has a constant value, $1/T$ (cf. definition of temperature), this can also be accomplished when the total derivative of $S(x) - E(x)/T \equiv -F(x, T)/T$ with respect to x vanishes (cf. definition of the free energy); in other words, maximization of $S(x)$ under the constraint $E(x) = const$ is equivalent to an unconditional minimization of $F(x, T) = E(x) - TS(x)$ at a given T.

for the function to be minimized. The thermodynamic quantities are the values of the above functions at the minimum $\bar{R}$.

Collecting the various terms, we obtain

$$
\begin{aligned}
F(T,R) &= -Nz\eta(R)\left(\bar{K}+\frac{\Delta K^2}{2T}\right) - NT\ln\nu_0 - 2T\ln\left(\frac{R}{R_0}\right) \\
&+ \frac{3}{2}T\left(\frac{R}{R_0}\right)^2 + NT\left[\frac{1-\eta(R)}{\eta(R)}\ln\left(1-\eta(R)\right)-1\right] \quad (2.25)
\end{aligned}
$$

Eq. (2.25) is typical of mean-field polymer collapse theories. It is general, in the sense that it makes no restriction to a loose packing fraction $\eta << 1$. For small η the theory simplifies; we will use this simplified form in what follows, because it gives results in closed form; those results however are only valid if they satisfy this criterion self-consistently, i.e. $\eta(\bar{R}) << 1$. (cf. exercise for more general numerical treatment).

For $\eta << 1$ the last term in (2.25) becomes $\eta/2 - \eta^2/6$; the linear term can be combined with the first term to give

$$
\left[\frac{T}{2} - z\left(\bar{K}+\frac{\Delta K^2}{2T}\right)\right]N\eta \quad (2.26)
$$

where the brackets in the above expression can be rewritten as $\frac{1}{2}(1+\Delta T/T)(T-T_\Theta)$, with $T_\Theta = z\bar{K}+\sqrt{z^2\bar{K}^2+z\Delta K^2}$ and $\Delta T = \sqrt{z^2\bar{K}^2+z\Delta K^2}-z\bar{K}$. Note that $\Delta T = 0$ if $\Delta K^2 = 0$, therefore the theory can describe the nonrandom (homopolymer) case as well.

In the new notation, the small η limit of F can be written as

$$
\begin{aligned}
F(T,R) &= -NT\ln\nu_0 - 2T\ln\left(\frac{R}{R_0}\right) + \frac{3}{2}T\left(\frac{R}{R_0}\right)^2 \quad (2.27) \\
&+ \frac{1}{2}\left(1+\frac{\Delta T}{T}\right)(T-T_\Theta)N^2\left(\frac{\sigma}{R}\right)^3 + NT\cdot\frac{1}{6}N^2\left(\frac{\sigma}{R}\right)^6 .
\end{aligned}
$$

Minimization of (2.27) gives

$$
\begin{aligned}
0 = \frac{\partial F}{\partial R} &= -2\frac{T}{R} + 3T\frac{R}{R_0^2} \\
&- \frac{3}{2}\left(1+\frac{\Delta T}{T}\right)(T-T_\Theta)N^2\frac{\sigma^3}{R^4} - T\cdot N^3\frac{\sigma^6}{R^7} . \quad (2.28)
\end{aligned}
$$

It is possible to obtain leading-order asymptotic solutions of (2.28) as $N >> 1$, $\bar{R} \propto N^\nu$ by examining the order of the various terms; they are:

$$
\begin{array}{cc}
Term & order \\
1 & N^{-\nu} \\
2 & N^{\nu-1} \\
3 & N^{2-4\nu} \\
4 & N^{3-7\nu}
\end{array} \quad (2.29)
$$

Note that the second term is larger than the first if $\nu > 1/2$, and the third term is larger than the fourth if $\nu > 1/3$. We distinguish 3 cases.

18

(i) uncollapsed solutions: If we look for solutions with $\nu > 1/2$, it is sufficient to keep the second and third terms. This gives positive solutions

$$\bar{R} = \left\{ \frac{\sigma^3}{2l^3} \left(1 + \frac{\Delta T}{T} \right) \left(\frac{T - T_\Theta}{T} \right) \right\}^{1/5} N^{3/5} l \tag{2.30}$$

if $T > T_\Theta$. At temperatures far higher than both T_Θ and ΔT, these uncollapsed solutions reduce to the result (2.13) determined by geometry alone.

(ii) collapsed solutions: we note that the third term is larger than the first if $\nu < 2/3$. Then if we look for solutions with $\nu < 1/2$, it is sufficient to keep the third and fourth terms. This gives positive solutions

$$\bar{R} = \left\{ \frac{3}{2} \left(1 + \frac{\Delta T}{T} \right) \left(\frac{T_\Theta - T}{T} \right) \right\}^{-1/3} N^{1/3} \sigma \tag{2.31}$$

if $T < T_\Theta$; the corresponding packing fraction is

$$\eta(\bar{R}) = N \left(\frac{\sigma}{\bar{R}} \right)^3 = \frac{3}{2} \left(1 + \frac{\Delta T}{T} \right) \left(\frac{T_\Theta - T}{T} \right) \tag{2.32}$$

i.e. the state is indeed compact, with packing fraction of order N^0; on the other hand, as long as the temperature stays in the approximate vicinity of T_Θ, the packing fraction remains much smaller than unity; therefore the self-consistency of the theory is guaranteed (cf. above) in the vicinity of the Θ-point.

(iii) the marginal case: at $T = T_\Theta$ the third term vanishes; the resulting equation

$$3 \left(\frac{R}{R_0} \right)^8 - \left(\frac{R}{R_0} \right)^6 = \left(\frac{\sigma}{l} \right)^6 \tag{2.33}$$

always has a solution of the form $\bar{R}/R_0 = f(\sigma/l)$. The solution is uncollapsed, yet less extended than the geometrical (2.13); it is of order $N^{1/2}$ (as the Gaussian random walk; but note that the prefactor is not the same).

Note that the approximate solutions given above for $\bar{R}(T, N)$ in cases (i) and (ii) above cannot remain valid in the immediate vicinity of the theta point; this is obvious for example in the case (i), since $\bar{R}$) becomes increasingly collapsed-like; conversely, as we approach T_θ from below, the solution (2.30) "opens up" in more and more. It is possible to invoke concepts of homogeneity and scaling (Exercise ..) to find solutions which describe the asymptotic behavior of $\bar{R}(T, N)$ arbitrarily close to the critical point. A useful corollary of this generalization is that the entropy is a continuous function of the temperature, i.e. there is no latent heat connected with the phase transition.

2.3 Application to proteins

Combinatorics:
No of conformations for each monomer:

$$\nu_0 = \nu + 1 \tag{2.34}$$

-one "native", rest non-native-. (Note: the number ν should not be confused with the critical exponent ν used in the previous section).

Consider a protein with N monomers. Of these, ρN are in the folded state and $(1-\rho)N$ in the non-folded state. (macroscopic description of the degree of order; use the language of phase transitions; ρ is in this sense an order parameter; in particular $\rho = 1$ corresponds to the completely folded state.).

Modify heteropolymer theory by considering the different conformational freedom of native and non-native residues. A nonnative residue can assume ν conformations. A native only one. And the number of ways we can select ρN natives and $(1-\rho)N$ nonnatives provides an additional conformational freedom for nonfolded states. Instead of the simple ν_0^N factor, we now have a total of

$$C(N, \rho) = \frac{N!}{(N\rho)![N(1-\rho)]!}\nu^{N(1-\rho)} \qquad (2.35)$$

coarse grained conformations for an N-monomer protein. Note that $C(N, 1) = 1$; the completely folded state has no conformational degrees of freedom. The number of conformations of an N-monomer protein with folding fraction ρ and end-to-end distance between R and $R + dR$ is now

$$\Omega^*(R, \rho)dR = \omega_{E.V.}C(N, \rho)P(R) \qquad (2.36)$$

and, after straightforward computations (Stirling appr.),

$$
\begin{aligned}
S^*(R, \rho) &= \ln \Omega^* \\
&= N\left[(1-\rho)\ln\nu - (1-\rho)\ln(1-\rho) - \rho\ln\rho\right] \\
&- N\left[\frac{1-\eta}{\eta}\ln(1-\eta) + 1\right] \\
&+ 2\ln\frac{R}{R_0} - \frac{3}{2}\left(\frac{R}{R_0}\right)^2 \qquad (2.37)
\end{aligned}
$$

Energetics:
Proteins are different from other heteropolymers in that they are "engineered" to fold into a particular (native) structure. In order for this to happen, different interactions must have a tendency to reinforce each other.
(Observation: lots of secondary structure present)
concept: *minimal frustration*
(should tend to favor ordered state rather than "protein glass").
Simple model:

- associate an energy $-\epsilon$ with each residue in native conformation. (zero if in non-native conformation).
  ("primary structure energy": not really an interaction (on-site term); however, it favors conformations with the right sequence, which will eventually fold). This contributes

  $$E_{primary}(\rho) = -N\rho\epsilon \qquad (2.38)$$

  to the total energy of the protein (straightforward and exact: there are ρN residues in folded state).

- associate an energy $-J$ with each residue if it *and* its predecessor are in native conformation. (zero if not)

("secondary structure energy": favors ordering at a local level). This contributes, in the m.f. approximation

$$E_{secondary}(\rho) = -N\rho^2 J \qquad (2.39)$$

(for each residue in folded state, probability ρ that the predecessor will also be in folded state).

- describe the overall hydrophobic effect in a fashion which favors folding: Modify the interactions of heteropolymer if *both* partners are in folded state; the energy is then -K (with no spread) rather than -$\bar{K}$. On the average, each interacting pair contributes $-\rho^2 K - (1-\rho^2)\bar{K}$. The average number of interactions is as in the heteropolymer case, $I(R) = z\eta(R)N$. This gives

$$\begin{align} E_{tertiary}(R,\rho) &= -I(R)\left[K + (1-\rho^2)\bar{K}\right] & (2.40) \\ \Delta E^2(R) &= I(R)(1-\rho^2)\Delta K^2. & (2.41) \end{align}$$

The total m.f. energy $\bar{E}(R,\rho)$ is the sum of the 3 terms above (primary, secondary, tertiary).

Eq. (2.41) represents all fluctuations. There is no other randomness.

carry on with heteropolymer program:
however, note that the variables ρ and R are not really independent. As the protein folding fraction increases, the overall structure generally becomes more compact, i.e. R should decrease. If η_f is the packing fraction of the folded protein (typically: 0.75)

$$R \sim \left(\frac{N}{\eta_f}\right)^{1/3} \sigma \ , \ (\rho \to 1) \ . \qquad (2.42)$$

Conversely, as the protein unfolds completely, its size tends to follow the 3/5 law:

$$R \sim 2^{-1/5}\left(\frac{\sigma}{l}N\right)^{3/5} l \ , \ (\rho \to 0) \ . \qquad (2.43)$$

If we minimize independently with respect to ρ and R, unphysical solutions may occur. "Radical" assumption: interpolate between the two extreme cases.

$$\begin{align} R(\rho) &= 2^{-1/5}\left[\frac{\sigma}{l}N(1-\rho)\right]^{3/5} l \ , \ 0 \le \rho < \rho_f & (2.44) \\ &= \left(\frac{N}{\eta_f}\right)^{1/3} \sigma \ , \ 0 \le \rho_f \le 1 & (2.45) \end{align}$$

where ρ_f is determined by the demand of continuity,

$$\rho_f = 1 - \left(\frac{2\sigma^2}{l^2}\right)^{1/3}\frac{1}{N^{4/9}\eta_f^{5/9}} \qquad (2.46)$$

and is interpreted as the fraction of residues which are in their native state in a folded protein which fluctuates in solution. Typical values $\eta_f = 0.75, N = 150, \sigma = l/\sqrt{2}$, give $\rho_f = 0.9$ (reasonable).

The proposed interpolation, although not exact, makes sense qualitatively: the non-native portion of the protein does a self-avoiding-random-walk and dominates the size for most values of ρ (except those which approach the folded state).

We now proceed with minimization with respect to a single variable, ρ. The number of states with energies in the interval $(E, E + dE)$ is given by

$$n(E)dE = \int_0^1 d\rho \, g(\rho, E) \Omega^*(\rho) \tag{2.47}$$

where the probability of finding a given energy E (at a particular ρ) is

$$g(\rho, E) = \frac{1}{\sqrt{2\pi \Delta E^2(\rho)}} e^{-\frac{[E - \bar{E}(\rho)]^2}{2\Delta E^2}} . \tag{2.48}$$

Again, the idea is that the integrand of Eq. (2.47), denoted as $e^{S(\rho, E)}$, should have a sharp maximum with respect to ρ, which will dominate the integration. Neglecting logarithmic terms,

$$S(\rho, E) = S^*(\rho) - \frac{\left[E - \bar{E}(\rho)\right]^2}{2\Delta E^2} . \tag{2.49}$$

Again, rather than finding the maximum of $S(\rho, E)$ at a given E (microcanonical), we perform a Legendre transform, and look for the minimum of the free energy at a constant temperature (canonical):

Thermodynamic definition of temperature

$$\left(\frac{\partial S}{\partial E}\right) = \frac{1}{T} , \tag{2.50}$$

Use (2.49) in (2.50) to obtain

$$E(T, \rho) = \bar{E}(\rho) - \frac{\Delta E^2(\rho)}{T} \tag{2.51}$$

and (2.51) in (2.49) to obtain

$$S(T, \rho) = S^*(\rho) - \frac{\Delta E^2(\rho)}{2T^2} . \tag{2.52}$$

The free energy function to be minimized is

$$\begin{aligned} F(T, \rho) &= E(T, \rho) - TS(T, \rho) \\ &= \bar{E}(\rho) - \frac{\Delta E^2(\rho)}{2T} - TS^*(\rho) . \end{aligned} \tag{2.53}$$

In collecting the various terms which contribute to (2.53), note that both the tertiary energy (included the first term) and the fluctuations (second term) contribute terms proportional to $-Nz\eta$. The proportionality constants are $\rho^2 K + (1 - \rho^2)\bar{K}$ from the tertiary term and $(1 - \rho^2)\Delta K^2/(2T)$ from the fluctuations term. This suggests defining a temperature-dependent function

$K_1(T) = \bar{K} + \Delta K^2/(2T)$, to combine the two contributions. The result is

$$
\begin{aligned}
F(T,\rho) &= -N\rho\epsilon - N\rho^2 J - Nz\eta(\rho)\left[K_1(T) + \rho^2(K - K_1(T))\right] \\
&\quad + NT\left[(1-\rho)\ln\frac{1-\rho}{\nu} + \rho\ln\rho + \frac{1-\eta}{\eta}\ln(1-\eta) + 1\right] \\
&\quad - 2T\ln\frac{R}{R_0} + \frac{3}{2}T\left(\frac{R}{R_0}\right)^2 .
\end{aligned}
\tag{2.54}
$$

For typical values $N = 150, z = 2, \epsilon = 0.1, J = 2.0, K = 0.6, \bar{K} = 0.3, \Delta K^2 = 0.2$ and $\eta_f = 0.75, \sigma = l/\sqrt{2}$ ($\rho_f = 0.9$, cf. above) one obtains at $T = 1$ a double-well potential. The absolute minimum near ρ_f corresponds to the folded state. The other minimum is at relatively low ρ (semicompact states). The transition is first order (cf. exercise). As the temperature increases, the low-folding-fraction minimum becomes stable. The protein is more likely to be found in semicompact conformations (*thermal denaturation*).

Protein glass: In principle, it is possible, particularly if the disorder is high, for the entropy to become negative. As the entropy approaches zero from above, the system experiences an "entropy crisis". For protein folding to proceed properly, the "entropy crisis" (*freezing, transition to a glassy state*) should occur at much lower temperatures (cf. exercise, compute entropy as a fn. of T). "Freezing" is defined by the vanishing of the right-hand-side of (2.52), which suggests that

$$
T_{fr}^2 = \frac{\Delta E^2(\bar{\rho})}{2S^*(\bar{\rho})}
\tag{2.55}
$$

where the bar means that the folding fraction should be determined self-consistently by minimization of the free energy at $T = T_{fr}$. From the point of view of un-inhibited folding, one would like to "guarantee" that freezing does not compete with collapse, i.e. $T_{fr} << T_\Theta$.

2.4   Kinetics of protein conformations

[Ref. Bryngelson & Wolynes, *J. Phys. Chem.* **93**, 6902 (1989)]
Description of "energy landscape" (local minima): analogies to theory of complex chemical reactions.
starting point: enumeration of residues found in native and nonnative conformations; number of possible conformations $C(N,\rho)$ (cf previous section).and its logarithm

$$
S^*(\rho) = \ln C(N,\rho) .
\tag{2.56}
$$

Geometry at this stage not explicit
Energy distribution: Gaussian (2.48).
Classification of states according to their number of native residues helps formulate the question of "which states are connected to a given state". We restrict transitions to those involving conformational changes of a *single* amino acid. Such changes can happen in νN ways, i.e. each conformation is "connected" to νN others. The following table shows schematically how a state with ρN native residues is connected to states with "neighboring" states "connected" with it. Changes of type $\Downarrow$ take a native residue and transform it to a nonnative; changes of type $\Uparrow$ take a nonnative residue and transform it to a native; finally, changes

of type $\Rightarrow$ take a nonnative residue and transform it to a different nonnative, without changing the overall number of native residues.

# of native residues	type of transition	# of paths
$\rho N + 1$		
	$\Uparrow$	$(1 - \rho)N$
ρN	$\Rightarrow$	$(1 - \rho)(\nu - 1)N$
	$\Downarrow$	$\rho N \nu$
$\rho N - 1$		
		νN

Local minima (definition): a state of energy E_0 is a local minimum (LM) if all $N\nu$ states connected to it have a higher energy. Probability for this

$$P_{LM}(E_0, \rho) = \left[\int_{E_0}^{\infty} dE\, g(E, \rho) \right]^{N\nu} \tag{2.57}$$

where the quantity in the brackets represents the probability that *any one* of the connected states has an energy higher than E_0. This assumes that, although individual energy changes can be large, the density of states does not change appreciably during conformational flips.

It is possible to integrate (2.57) over the energy distribution in order to obtain the probability that any given conformation, independently of its energy, is a local minimum. The integral

$$p_{LM}(\rho) = \int_{-\infty}^{\infty} dE_0\, P_{LM}(E_0, \rho)\, g(E, \rho) \tag{2.58}$$

is of the form

$$-\int_{-\infty}^{\infty} dx\, \phi'(x)\phi^m(x) = \frac{1}{m+1} \tag{2.59}$$

with $\phi(x) \equiv \int_{x}^{\infty} dx'\, g(x')$, and the evaluation has been done using the properties $\phi(\infty) \equiv 0$ and $\phi(-\infty) = 1$ (normalization). This leads to a probability

$$p_{LM} = \frac{1}{N\nu + 1} \tag{2.60}$$

independent of the number of native residues. The average number of local minima can now be found to be

$$\begin{aligned}
< n_{LM} > &= \sum_{\rho N = 0}^{N} C(N, \rho)\, p_{LM} \\
&= \frac{(1 + \nu)^N}{1 + \nu N} .
\end{aligned} \tag{2.61}$$

The last statements about conformational space are independent of the details of the energy distribution. The number of local minima is still astronomical; however, for $\nu = 10, N = 100$ it represents only .1% of all states. We expect the deeper minima to be of significance (kinetic traps, misfolded structures, folding intermediates).

Statement about energy distribution of local minima?

We know the total number of LM, the probability that a state of given energy is a LM, and the overall distribution of energies. The normalized energy distribution of LM is given by

$$g_{LM}(E_0, \rho) = (N\nu + 1)\, g(E_0, \rho)\, P_{LM}(E_0, \rho)\,. \qquad (2.62)$$

To obtain a more useful form of (2.62), note that the brackets in (2.57) can be written as

$$
\begin{aligned}
\int_{E_0}^{\infty} dE\, g(E, \rho) &= \int_{-\infty}^{\infty} dE\, g(E, \rho) - \int_{-\infty}^{E_0} dE\, g(E, \rho) \\
&= 1 - \int_{-\infty}^{E_0} dE\, g(E, \rho) \\
&\approx e^{-\int_{-\infty}^{E_0} dE\, g(E, \rho)}
\end{aligned}
\qquad (2.63)
$$

provided that the remaining integral is in some sense (to be made precise below) much smaller than unity. Note that if this is not the case, raising it to a very high power (cf (2.57)) will make the r.h.s of (2.62) vanish. We now define a "threshold energy" via

$$\int_{-\infty}^{E_c(\rho)} dE\, g(E, \rho) = \frac{1}{N\nu}\,. \qquad (2.64)$$

We can now make a rough estimate of the r.h.s of (2.62) as follows: If the argument of the exponential in P_{LM} (including the $N\nu$ factor) is smaller than unity we set the exponential equal to one; if it is larger than unity we set the exponential equal to zero. This results in the approximate energy distribution of LM

$$
\begin{aligned}
g_{LM}(E_0, \rho) &\approx \frac{N\nu}{\sqrt{2\pi \Delta E^2(\rho)}} e^{-\frac{[E_0 - \bar{E}(\rho)]^2}{2\Delta E^2}} \quad (if\ E_0 < E_c(\rho)) \\
&\approx 0 \quad (if\ E_0 > E_c(\rho))\,.
\end{aligned}
\qquad (2.65)
$$

The value of the threshold can be obtained from the leading-order asymptotics of the error function and is given by

$$E_c(\rho) = \bar{E}(\rho) - [2\ln(N\nu)]^{1/2}\, \Delta E(\rho) \qquad (2.66)$$

Eqs. (2.65) and (2.66) are very strong statements about local minima. The approximate distribution function states that there are no LM in appreciable numbers above E_c; on the other hand, the threshold E_c itself is in the tail of the Gaussian energy level distribution: for $N = 100$ (relatively small) and $\nu = 10$, $[2\ln(N\nu)]^{1/2} = 3.7$. Furthermore, because P_{LM} is approximately equal to unity if the energy is below threshold, essentially *all* energy levels below E_c are local minima.

The state of lowest energy can be estimated from the condition

$$g(E_{low}(\rho)) = \frac{1}{C(N, \rho)} \qquad (2.67)$$

which expresses the probability of finding an isolated state. This leads to

$$E_{low}(\rho) = \bar{E}(\rho) - [2S^*]^{1/2}\,\Delta E(\rho) \tag{2.68}$$

Kinetics; escape rate from a LM: we use Metropolis (Monte Carlo, MC) kinetics. The transition from state A to state B takes place with a rate

$$\Gamma_{AB} = \begin{cases} \Gamma_0 e^{-\beta(E_B - E_A)} & \text{if } E_B > E_A \\ \Gamma_0 & \text{if } E_B < E_A \end{cases} \tag{2.69}$$

Total escape rate from E_0:

$$\begin{aligned} \bar{\Gamma}(E_0, \rho) &= \Gamma_0 \sum_{\{i\} \text{ connected to LM}} e^{-\beta(E_i - E_0)} \\ &= \Gamma_0 \nu N \, \frac{\int_{E_0}^{\infty} dE \, g(E, \rho) \, e^{-\beta(E - E_0)}}{\int_{E_0}^{\infty} dE \, g(E, \rho)} \end{aligned} \tag{2.70}$$

where the denominator has been introduced in order to provide the correct normalization, since we only integrate over states with energies above E_0. In fact, we have already proved that the denominator in (2.70) is unity (within our estimation scheme), since all LM are in the tail of the Gaussian.

We still have to calculate the integral

$$I(E^0) = \frac{1}{\sqrt{2\pi}\Delta E} \int_{E_0}^{\infty} dE \, e^{f(E)} \tag{2.71}$$

where

$$\begin{aligned} f(E) &= -\frac{(E - \bar{E})^2}{2\Delta E^2} - \beta(E - E_0) \\ &= f(E_m) - \frac{1}{2\Delta E^2}(E - E_m)^2 \end{aligned} \tag{2.72}$$

and in the second line we have written f in terms of its maximum value

$$f(E_m) = -\beta(\bar{E} - E_0) + \frac{1}{2}(\beta\Delta E)^2 \tag{2.73}$$

at

$$E_m = \bar{E} - \beta\Delta E^2 \,. \tag{2.74}$$

We distinguish two cases:

I. If $E_m > E_0$ or, equivalently,

$$E_0 < \bar{E} - \beta\Delta E^2 \tag{2.75}$$

the maximum falls inside the integration region. The integral is approximated by $\exp[f(E_m)]$ and the result is

$$\bar{\Gamma}_I(E_0, \rho) = \nu N \, \Gamma_0 \, e^{-\beta(\bar{E} - E_0) + \frac{1}{2}(\beta\Delta E)^2} \tag{2.76}$$

Note that (by definition) $E_0 > E_{low}$, and therefore, from (2.68) and (2.75) the double inequality

$$\beta\Delta E^2 < \bar{E} - E_0 < (2S^*)^{1/2}\Delta E \tag{2.77}$$

holds; hence in case (I)

$$T > T_{low}(\rho) \equiv \frac{\Delta E(\rho)}{(2S^*)^{1/2}} \tag{2.78}$$

must hold; if $T < T_{low}(\rho)$ there is no contribution to the decay rate from case (I).

II. If $E_m < E_0$ or, equivalently,

$$E_0 > \bar{E} - \beta\Delta E^2 \tag{2.79}$$

the maximum falls outside the integration region. Note first that since $E_0 < E_c$ (cf. above), now the double inequality

$$\beta\Delta E^2 > \bar{E} - E_0 > [2\ln(N\nu)]^{1/2}\Delta E \tag{2.80}$$

holds; hence in case (II)

$$T < T_{high}(\rho) \equiv \frac{\Delta E(\rho)}{[2\ln(N\nu)]^{1/2}} \tag{2.81}$$

must hold; if $T > T_{high}(\rho)$ there is no contribution to the decay rate from case (II).

An estimate of the integral (2.71) can now be obtained as follows: The integrand is a product of an exponential, peaked at $E - E_0$ and with a width T, and the Gaussian from the energy density of states. From (2.81), T is significantly smaller than ΔE, thus the peaks of the two functions are well separated (cf Fig). This allows us to set $E \approx E_0$ in the Gaussian and pull it out of the integral; the result is a Gaussian

$$\bar{\Gamma}_{II}(E_0,\rho) = \nu N \, \Gamma_0 \, e^{-\frac{1}{2}\left(\frac{E_0 - \bar{E}}{\Delta E}\right)^2} \tag{2.82}$$

where the prefactor has been fixed by the requirement of continuity at $E_0 = E_m$.

In summary, the average escape rate from a LM is a monotonic function of the LM energy

$$\bar{\Gamma}(E_0, \rho) = \begin{cases} \bar{\Gamma}_I(E_0, \rho) \; if \; E_0 \leq \bar{E} - \beta\Delta E^2 \\[2mm] \bar{\Gamma}_{II}(E_0, \rho) \; if \; E_0 \geq \bar{E} - \beta\Delta E^2 \end{cases} \tag{2.83}$$

At $E_0 = \bar{E} - \beta\Delta E^2$ it follows from either alternative that

$$\bar{\Gamma}(\bar{E} - \beta\Delta E^2, \rho) = \nu N \, \Gamma_0 \, e^{-\frac{1}{2}\left(\frac{\Delta E}{T}\right)^2} \equiv \Gamma^*(\rho) \,. \tag{2.84}$$

Note further that (i) escape rates must be in the interval $(\Gamma_{min}, \Gamma_{max})$, where

$$\Gamma_{min}(\rho) = \bar{\Gamma}(E_{low}, \rho) = \nu N \, \Gamma_0 \, e^{-(2S^*)^{1/2}\beta\Delta E + \frac{1}{2}\beta^2\Delta E^2} \tag{2.85}$$

$$\Gamma_{max}(\rho) = \bar{\Gamma}(E_c, \rho) = \Gamma_0 \tag{2.86}$$

and (ii) at the special temperatures $T_{high}(\rho)$ and $T_{low}(\rho)$ the following relationships hold, respectively

$$\Gamma_{min}(\rho) = \Gamma^*(\rho) = \nu N \Gamma_0 e^{-S^*} \; [\; at \, T = T_{low}(\rho)] \tag{2.87}$$

$$\Gamma_{max}(\rho) = \Gamma^*(\rho) = \Gamma_0 \, [at \, T = T_{high}(\rho)] \,. \tag{2.88}$$
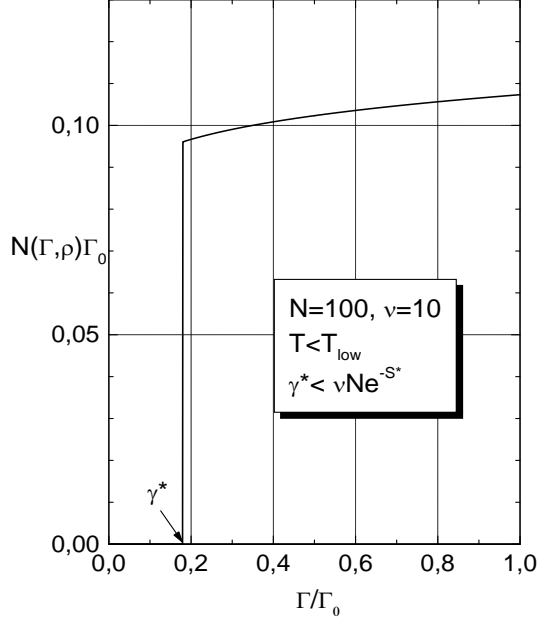
Figure 2.1: A typical "flat" distribution of escape rates for $T < T_{low}$ according to Eq. (2.91b). The temperature enters only via the lower cutoff $\gamma^* \equiv \Gamma^*/\Gamma_0$.

Distribution of escape rates: Let $\mathcal{N}(\Gamma)d\Gamma$ be the number of LM with escape rates in the interval $(\Gamma, \Gamma + d\Gamma)$. We can write

$$\mathcal{N}(\Gamma, \rho) = \int_{-\infty}^{+\infty} dE_0 \, g_{LM}(E_0) \, \delta\left[\Gamma - \bar{\Gamma}(E_0, \rho)\right] \tag{2.89}$$

$$= \frac{g_{LM}(E_0)}{\left|\frac{\partial \bar{\Gamma}(E_0, \rho)}{\partial E_0}\right|_{\bar{\Gamma}(E_0, \rho) = \Gamma}} . \tag{2.90}$$

A straightforward calculation (Exercise ..) yields

$$\mathcal{N}(\Gamma, \rho) = \begin{cases} (2\pi)^{-1/2} \frac{T}{\Gamma_0 \Delta E} e^{-\frac{1}{2}\left\{\frac{T}{\Delta E} \ln \frac{\Gamma}{\Gamma^*}\right\}^2} & \text{if } \Gamma_{min} < \Gamma < \Gamma^* \\ (2\pi)^{-1/2} \frac{1}{\Gamma_0} \frac{1}{\sqrt{2 \ln\left(\frac{\nu N \Gamma_0}{\Gamma}\right)}} & \text{if } \Gamma^* < \Gamma < \Gamma_{max} \end{cases} \tag{2.91}$$

The purist will note that $\mathcal{N}(\Gamma, \rho)$ is discontinuous at Γ^*; the discontinuity reflects the discontinuity of the derivative of $\bar{\Gamma}(E_0)$ at $E_0 = E_m$.

Discussion: If we look at the slowest escape rate, Γ_{min} as a function of temperature, we note that it has a *minimum* at $T = T_{low}$. (interpretation: *dynamical freezing transition* occurs at the same temperature as the freezing predicted by the mean-field equilibrium theory). For temperatures $T < T_{low}$,

28

the distribution is given solely by the form (II) [since $\Gamma^* < \Gamma_{min}$ there is no region I] and is very broad, characteristic of the glassy state (cf. Fig. 2.1). Long relaxation times are almost equally probable with short relaxation times.

In the intermediate temperature regime $T_{high} > T > T_{low}$, both Γ regions are present. Faster rates are distributed according to II (broad), slower rates according to I (cf. Fig. 2.2). Very slow rates are inhibited by the exponential in I, i.e. they are not favored. This is important from the point of view of protein folding. Kinetic traps created by local minima with long escape rates should not be prevalent along the folding path, since they would create a "bottleneck".
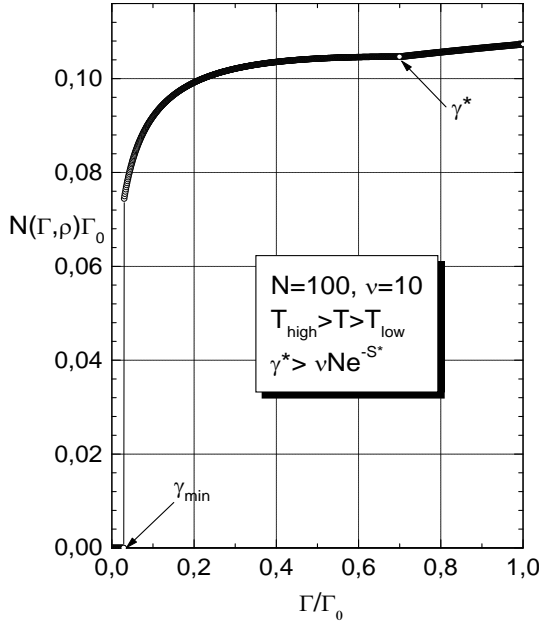

Figure 2.2: Typical distribution of escape rates at intermediate temperatures. Both cases of Eq. (2.91) contribute. Very slow rates are suppressed by the form of (2.91a).

A final note: The absolute minimum of relaxation rates which occurs at T_{low} represents the entropy crisis from a dynamical viewpoint. Rewriting (2.87) as

$$\Gamma^*(T_{low}) = \nu N \Gamma_0 \, e^{-S^*} = \frac{\nu N \Gamma_0}{\Omega^*} \tag{2.92}$$

we note first by a formal comparison with the Arrhenius expression *rate* $\propto e^{\Delta S - \beta \Delta H}$ that a huge negative entropy controls the escape rate at this extremum; alternatively, we use the second expression in order to identify a *longest escape time*

$$\tau^*_{max} = \frac{1}{\Gamma^*(T_{low})} = \frac{1}{\Gamma_0} \frac{1}{\nu N} \Omega^* \tag{2.93}$$

In a sense this is the "Levinthal catastrophe": all paths must be sequentially explored.

A detailed, semiquantitative theory of the folding process has been developed by Bryngelson and Wolynes using the concepts developed above. Although the technical part is slightly beyond the scope of these lectures, its rationale is relatively straightforward. A protein state with a given folding fraction, is considered as a "kinetic trap", for which the concept of a continuous time random walk (CTRW, Montroll & Weiss, J. Math. Phys. **6**, 167(1965)) is applicable. What this says, in a nutshell, is that the protein performs a diffusion in ρ-space, driven by the thermodynamic potential, which is roughly described by the effective free energy at a given ρ and T. Folding is thus described as a driven diffusion process, which starts at a state of low ρ, escapes the kinetic traps and eventually enters the $\rho = \rho_f$ state. In statistical physics, this is cast in the form of a "first passage time" problem. I will deal with a simpler case of such a problem in a later lecture.

Chapter 3

Phase transitions in biopolymers

3.1 Introductory remarks

Examples:

1. protein unfolding of 3d structures
   ribonuclease (reversible)

2. DNA "melting": separation of the two strands of the double helix

3. synthetic polypeptide chains. Breakup into ordered (helical) and disordered (coiled) regions. Ideal for studying the properties of secondary structure.

We have discussed some aspects of (1) in the previous chapter. here: 2 and 3, with complementary theoretical approaches. Will use (3) as starting point. Language more physico-chemical; in (2) modern statistical physics. Physicists should not "look down" on type (3) formalism. This is the language of experiments! Ideally, approaches should be complementary and translatable.

$$physical\ chemistry \qquad \longleftrightarrow \qquad physics$$
$$statistical\ mechanics$$

3.2 Helix-Coil transitions

residues in helical regions give rise to optical rotation. At given N (controlled in synthetic polypeptides) one can measure the helix fraction. Typically, that fraction completes the transition from 1 to 0 over a fairly narrow temperature range (a few degrees K in the case of long chains). Chemists describe the process

$$A \quad \longleftrightarrow \quad B \tag{3.1}$$
$$(helix) \qquad (coil) \tag{3.2}$$

as an equilibrium between the two species,

$$K = \frac{c_B}{c_A} = e^{-\Delta G/(RT)} \tag{3.3}$$

where the helix fraction is given by

$$\Theta = \frac{c_A}{c_A + c_B} = \frac{1}{1 + K} \; . \tag{3.4}$$

Sign convention: We are looking at the conversion of helix (A) to coil (B). Therefore $\Delta G = G_B - G_A$, and ΔH (cf. below) is positive (the helix is energetically favored).

The value $\Theta = 0.5$ defined the midpoint of the transition, T_m. At that point, the apparent equilibrium constant $K = 1$. (Apparent because, it does not describe the microscopic states which contribute to the macroscopic observable).

If we write

$$\Delta G = \Delta H - T \Delta S \tag{3.5}$$

and assume (although this is not exact, and sometimes not even a good approximation) that the enthalpy and entropy differences do not depend very much on temperature, we obtain

$$\frac{d \ln K}{dT} = \frac{\Delta H}{RT^2} \tag{3.6}$$

and

$$\left(\frac{d\Theta}{dT} \right)_{\Theta = 0.5} = -\frac{1}{4} \frac{\Delta H}{RT^2} \; . \tag{3.7}$$

The inverse of Eq. (3.7) measures the width of the transition (in degrees K). A sharp transition (of a few degrees K) has a high [van't Hoff] ΔH (of the order of 100 Kcal/mol), indicating that perhaps as many as 100 hydrogen bonds are cooperatively broken during the transition.

Theoretical models (underlying ideas):

I. an *existing* helix may grow further at the *nth* site, or shrink. This is viewed as a forward and reverse reaction, with a rate ratio $s = \exp(-\Delta G^*/(RT))$, which reflects the difference in local free enrgies between the helix and coil states. If the ratio is greater than unity, the helix has a tendency to grow. If it is less than unity, the helix will shrink. At temperatures near the transition, $s = \mathcal{O}(1)$. The enthalpy difference ΔH^* corresponds to the energy of a single hydrogen bond formed or broken in the process.

II. *Nucleation* is a distinct process. In order to initiate a helix, 3 residues have to organize themselves. Again, viewing nucleation as a forward / reverse reaction, we can introduce a dimensionless $\sigma = \exp(-\Delta G_{init}/(RT))$. The large difference in the free energy comes mostly from the entropy loss associated with the organization of the 3-4 residues involved in the first turn of the helix.

Theoretical models (the particulars):
0 th order: The "all or nothing" (AON) model (mainly for completeness). Only two states are significant within this model. The pure coil, with relative statistical weight equal to unity; and the helix with N residues, with a relative
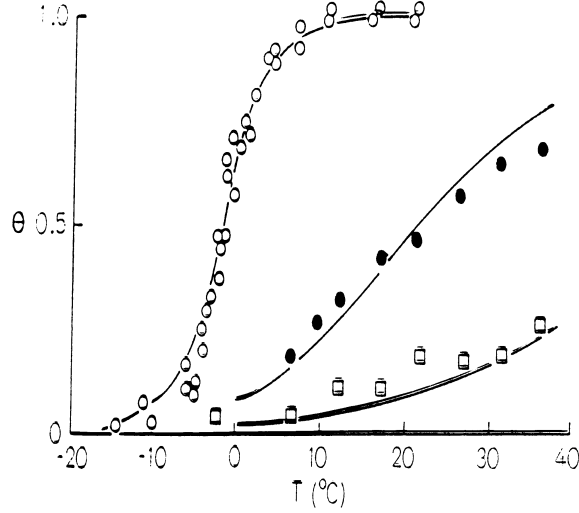
Figure 3.1: The helix-coil transitions in polypeptides of variable length , $\sqcap(N = 26), \bullet(N = 46), \circ(N = 1500)$ (after Doty et al, PNAS, **45**, 1601 (1959).

weight σs^N. Intermediate states are suppressed, presumably due to high rate barriers. This gives a helix fraction

$$\Theta = \frac{1}{N}\frac{N\sigma s^N}{1 + \sigma s^N} \tag{3.8}$$

and a slope at midpoint

$$\left(\frac{d\Theta}{dT}\right)_{\Theta=0.5} = -\frac{N}{4}\frac{\Delta H^*}{RT_m^2} \ . \tag{3.9}$$

There is strong cooperativity.

further considerations: The zipper model

The model allows a single connected helical region of any length $n \leq N$. The statistical weight (Boltzmann factor) is -according to the general considerations, cf. above-, σs^n, and the helix can commence at any of the first $A_n = N - n + 1$ positions. This gives a partition function

$$Z = 1 + \sum_{n=1}^{N} A_n \sigma s^n \tag{3.10}$$

and a helical fraction

$$\begin{aligned}
\Theta &= \frac{1}{Z}\sum_{n=1}^{N} n A_n \sigma s^n \\
&= \frac{1}{Z}s\frac{\partial Z}{\partial s} \\
&= \frac{\partial \ln Z}{\partial \ln s} \ . \tag{3.11}
\end{aligned}$$

33

The partition sum can be evaluated to give

$$Z(N) = 1 + \sigma s^{N+2} - (N+1)s + \frac{N}{(s-1)^2} \,. \tag{3.12}$$

The generalized zipper model

The only difference is topological: helical and coil regions may alternate without any further constraints. One associates the following weights:

1 if coil comes after helix or coil

s if helix comes after helix

σs if helix comes after coil (nucleation).

The model thus implements considerations (I) and (II) above, without imposing any further constraints. The state of the residue at site i can be described by a 2-vector ν_i, and the partition function is given by

$$
\begin{aligned}
Z_N &= \sum_{\{\nu_1\}...\{\nu_N\}} <\nu_1|T|\nu_2><\nu_2|T|\nu_3>...<\nu_{N-1}|T|\nu_N> \\
&= \sum_{\{\nu_1\},\{\nu_N\}} <\nu_1|T^N|\nu_N>
\end{aligned}
\tag{3.13}
$$

where the matrix elements of $\mathbf{T}$ express the Boltzmann factors specified above.

$$\mathbf{T} = \begin{pmatrix} s & 1 \\ \sigma s & 1 \end{pmatrix}. \tag{3.14}$$

To evaluate the partition sum, apply PBC (convenient, not a must); we obtain

$$Z_N = Tr\mathbf{T}^N = \lambda_0^N + \lambda_1^N \tag{3.15}$$

where the eigenvalues are given by

$$\lambda_{0,1} = \frac{1}{2}\left[1 + s \pm \Delta\right] \tag{3.16}$$

$$\Delta = \sqrt{(1-s)^2 + 4\sigma s} \tag{3.17}$$

and, in the lage N limit, Z is dominated by the largest eigenvalue, λ_0.

Note that the partition function (not the T-matrix) can be mapped onto the one of the ferromagnetic Ising model (exchange interaction J, magnetic field h, with the identifications

$$
\begin{aligned}
s &\Leftrightarrow e^{-2\beta h} & \tag{3.18} \\
\sigma &\Leftrightarrow e^{-2\beta J} & \tag{3.19} \\
\lambda_{magnetic} &= e^{\beta(J+h)}\lambda_{helix-coil} \,. & \tag{3.20}
\end{aligned}
$$

To obtain the helix fraction, note that if the probability of obtaining a helical segment of length k is given by $\phi_k(\sigma)ks^k$, where ϕ is the coefficient of s^k in the partition sum. This gives

$$
\begin{aligned}
\Theta &= \frac{1}{N}\frac{1}{Z}\sum_{k=1}^{N}\phi_k(\sigma)ks^k \\
&= \frac{1}{N}\frac{1}{Z}s\frac{\partial Z}{\partial s} \\
&= \frac{1}{N}\frac{\partial \ln Z}{\partial \ln s} \\
&\approx \frac{\partial \ln \lambda_0}{\partial \ln s} \,.
\end{aligned}
$$

One can now verify that as $s \to 1$, $\Delta \to 2\sqrt{\sigma}$, $\Theta \to 1/2$; for $\sigma << 1$ (cf. below), this gives

$$\left(\frac{d\Theta}{ds}\right)_{s=1} = \frac{1}{4\sqrt{\sigma}} \qquad (3.21)$$

or

$$\left(\frac{d\Theta}{dT}\right)_{\Theta=0.5} = -\frac{1}{4\sqrt{\sigma}} \frac{\Delta H^*}{RT_m^2} . \qquad (3.22)$$

i.e. the width of the transition is

$$\Delta T_m = 4\sqrt{\sigma} \frac{RT_m^2}{\Delta H^*} . \qquad (3.23)$$

Expt. by Doty et al (PNAS **45**, 1601 (1959)). Data for short (N=26,46) and long (N=1500) chains. Fits with $\sigma = 2 \times 10^{-4}$, $\Delta H^* = 4.14 kJ/mole$ (cf calorimetric measurements $\Delta H = 3.97 kJ/mole$). Interpret $1/\sqrt{\sigma}$ as number of residues cooperatively involved in the transition. (comparison with AON theory) follows also from Ising theory, since the inverse correlation length is given (in lattice constants) by

$$1/\xi = \lambda_1 - \lambda_0 = 2\sqrt{\sigma} \ \ (\text{at } s = 1) . \qquad (3.24)$$

Chemical language provides an independent estimate for $\sigma = e^{-\Delta G_{init}/RT} \approx e^{\Delta S_{init}/R}$: Initiation of the helix involves oraganization of J (=3,4) residues, each one by 2 dihedral angles. Typically a dihedral angle can take 3 independent orientations in space. This gives a total of 3^{2J} states, or an entropy loss $\Delta S_{init}/R = -2J\ln 3$. (J=3, 6.6; J=4, 8.8). This compares favorably with $\ln \sigma = 8.5$.

Similarly, one can relate the entropy loss involved in helix *growth*, to the energy of the H-bond. At the transition, $\Delta S^* = \Delta H^*/T_m = 1.85R$. This compares favorably with the estimate $2\ln 3 \approx 2.20$, obtained by considering the 2 dihedral angles which must be organized to admit a residue into the helix.

Theory in a sense "complete". reasonable assumptions, Well studied area. Many quantitative discrepancies. Enthalpies and entropies not constant etc. etc. The analysis depends very strongly on the Ising theory and therefore excludes the occurrence of an exact transition as $N \to \infty$ (even though the experimental evidence seems to support it). Physicist's more fundamental critique (and perhaps potential contribution): This is not what we understand in physics as a cooperative phenomenon. Point is not whether it is mathematically sharp or not; rounding always exists for a variety of reasons. Point is that statistical mechanics, as the physicist understands it, has a somewhat different agenda: Given some material-dependent but *T-independent* parameters of the Hamiltonian it sets out to predict material behavior *as a function of temperature*. Helix-coil theory does not do that.

3.3 Hamiltonian approach to DNA denaturation

The model [Peyrard & Bishop, *PRL* **62**, 2755 (1989); Theodorakopoulos, Dauxois & Peyrard, *ibid* **85**, 6 (2000)]:
Two parallel, harmonic chains, with lattice constant l, joined in the form of a ladder by anharmonic springs (H-bonds,modelled by a Morse potential) The
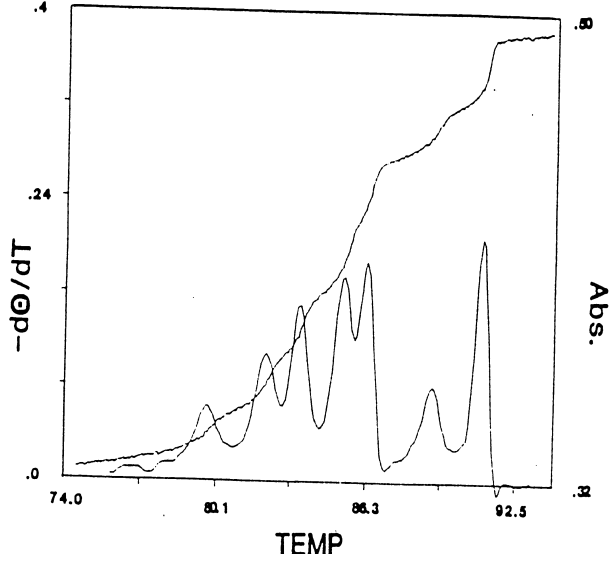
Figure 3.2: Absorbance vs temperature and differential melting curve for the 1630bp *Hinf* I restriction endonuclease DNA fragment of the pBR322 (cf Wartell & Benight, Phys. Repts **126**, 67 (1985)).

emphasis is on modelling the unbinding of the two chains, not the helical aspect of the ordered state. Lesson of theory of critical phenomena: "essentials" of the interactions completely determine the critical behavior. Identifying the essentials is of course a non-trivial issue when dealing with new phenomena.

$$H_{tot} = \frac{m}{2} \sum \left[\dot{u}_n^2 + \dot{v}_n^2 + \omega_0^2 \left(u_n - u_{n-1} \right)^2 + \omega_0^2 \left(v_n - v_{n-1} \right)^2 \right] + \sum_n V(u_n - v_n)$$

(3.25)

where

$$V(x) = D(e^{-ax} - 1)^2 .$$

(3.26)

We have assumed that the bases have equal masses and are connected by "transverse harmonic springs" of equal strength.

Transformation to CM and relative coordinates, $X_n = (u_n + v_n)/2, y_n = u_n - v_n, M = 2m, 1/\mu = 2/m$ decouples longitudinal from transverse Hamiltonian, i.e.

$$H_{tot} = H_0(X) + H(y)$$

(3.27)

where

$$H_0(X) = \sum_n \left[\frac{P_n^2}{2M} + \frac{1}{2} M \omega_0^2 (X_n - X_{n-1})^2 \right]$$

(3.28)

where $P_n = M\dot{X}_n$ is the canonical momentum conjugate to X_n, and

$$H(y) = \sum_n \left[\frac{p_n^2}{2\mu} + \frac{1}{2}\mu\omega_0^2(y_n - y_{n-1})^2 + V(y_n) \right] .$$

(3.29)

36

where $p_n = \mu \dot{y}_n$ is the canonical momentum conjugate to y_n.

H_0 is just the Hamiltonian of a harmonic chain with the total base pair mass per site. It gives an additive nonsingular contribution to all thermal properties. We will neglect in what follows.

Classical thermodynamics of H:

Canonical partition function

$$Z = \int d\Gamma e^{-\beta H} \tag{3.30}$$

where $d\Gamma$ is shorthand for the full set of canonically conjugate phase space coordinates, i.e.

$$d\Gamma = \prod_{n=1}^{N} dp_n dy_n . \tag{3.31}$$

One can immediately perform the Gaussian integrals over momentum space (this is the technical advantage of classical physics - no commutation problems to worry about!). Z splits into 2 factors

$$Z = Z_K Z_P, \tag{3.32}$$

where each integration in the kinetic part contributes a $(2\pi\mu/\beta)^{1/2}$ factor, i.e.

$$Z_K = (2\pi\mu/\beta)^{N/2} \tag{3.33}$$

to the partition function. The nontrivial part is

$$Z_P = \int \left(\prod_{n=1}^{N} dy_n \right) T(y_1, y_2) \cdots T(y_{N-1}, y_N) T(y_N, y_{N+1}) \tag{3.34}$$

where

$$T(x, y) = e^{-\beta \left[\frac{\mu \omega_0^2}{2}(y-x)^2 + V(x) \right]} \tag{3.35}$$

and can be evaluated as follows (Transfer integral method, note the conceptual analogy with the transfer matrix method of the Ising model):

Consider the eigenvalue problem defined by the asymmetric kernel T (the kernel can be easily symmetrized but we need not do so; in fact, working with the asymmetric kernel is technically advantageous in examining the validity of some approximations, cf. below):

$$\int_{-\infty}^{\infty} dy\, T(x, y)\, \Phi_\nu^R(y) = \Lambda_\nu \Phi_\nu^R(x) \tag{3.36}$$

$$\int_{-\infty}^{\infty} dy\, T(y, x)\, \Phi_\nu^L(y) = \Lambda_\nu \Phi_\nu^L(x), \tag{3.37}$$

where left and right eigenstates have been assumed to be normalized; note that the normalization integral is $\int dx \Phi_\nu^L(x)\Phi_\nu^R(x)$. Orthogonality

$$\int_{-\infty}^{\infty} dx\, \Phi_\nu^L(x)\, \Phi_{\nu'}^R(x) = \delta_{\nu\nu'} \tag{3.38}$$

and completeness

$$\sum_\nu \Phi_\nu^L(x)\,\Phi_\nu^R(y) = \delta(x-y) \tag{3.39}$$

relationships hold. We will further use the notation

$$\Lambda_\nu = e^{-\beta\epsilon_\nu} \tag{3.40}$$

(assumes nonnegative eigenvalues; this can be proved for the particular form of the kernel). Note further that the integrand of (3.34), as written down has a problem: it includes a reference to the displacement y_{N+1} of the $N+1st$ particle, which has not yet been defined. For a large system, this is best remedied by means of periodic boundary conditions (PBC), i.e. by demanding that $y_{N+1} = y_1$. Alternatively, we may extend the integration to one more variable, dy_{N+1}, and introduce a factor $\delta(y_{N+1} - y_1)$ to take care of PBC. This however is the same as the sum in the left-hand-side of (3.39). We then obtain

$$Z_P = \sum_\nu \int dy_1 \cdots \underbrace{dy_{N+1}\Phi_\nu^L(y_1)}\, T(y_1, y_2) \cdots \underbrace{T(y_N, y_{N+1})\Phi_\nu^R(y_{N+1})} \ . \tag{3.41}$$

The braces make clear that we can perform the integral over dy_{N+1} and obtain a factor $\Lambda_\nu \Phi_\nu^R(y_{N+1})$, using the defining property of right-hand eigenfunctions. The process can be repeated N times, each time giving a further factor Λ_ν and a right eigenfunction with an argument whose index is smaller by one. At the end, we are left with

$$\begin{aligned}
Z_P &= \sum_\nu \int dy_1 \Phi_\nu^L(y_1)\Lambda_\nu^N \Phi_\nu^R(y_1) \\
&= \sum_\nu \Lambda_\nu^N \ .
\end{aligned} \tag{3.42}$$

In the thermodynamic limit, Z_P is dominated by the largest eigenvalue Λ_0 or, equivalently, the lowest ϵ_0:

$$\lim_{N\to\infty} \frac{1}{N} \ln Z_P = \ln \Lambda_0 = -\beta\epsilon_0 \tag{3.43}$$

Other thermodynamic properties:
Order parameter:

$$\begin{aligned}
< y_i > &= \frac{1}{Z_P} \int dy_1 \cdots dy_N T(y_1, y_2) \cdots T(y_{i-1}, y_i) y_i \\
&\quad T(y_i, y_{i+1}) \cdots T(y_N, y_{N+1}) \\
&\equiv \frac{1}{Z_P} \sum_\nu \int dy_1 \cdots dy_{N+1} \Phi_\nu^L(y_1) \underbrace{T(y_1, y_2) \cdots T(y_{i-1}, y_i)}_{i-1} y_i \\
&\quad \underbrace{T(y_i, y_{i+1}) \cdots T(y_N, y_{N+1})}_{N-i+1} \Phi_\nu^R(y_{N+1}) \ ,
\end{aligned} \tag{3.44}$$

after insertion of a complete set of states (cf. above); the braces denote the number of times we can perform an integration and obtain, respectively, a right eigenfunction with an argument smaller by one, or a left eigenfunction with an

argument larger by one (as well as a factor Λ_ν. The remaining integral must be performed explicitly:

$$
\begin{aligned}
< y_i > &= \frac{1}{Z_P} \sum_\nu \Lambda_\nu^N M_{\nu\nu} \\
&\approx M_{00}
\end{aligned}
\tag{3.45}
$$

where the second line is exact in the thermodynamic limit, and we have used the abbreviation

$$
M_{\nu\mu} = \int_{-\infty}^{\infty} dy \Phi_\nu^L(y) y \Phi_\mu^R(y) \quad .
\tag{3.46}
$$

correlations $(i < j)$:

$$
\begin{aligned}
< y_i y_j > &\equiv \frac{1}{Z_P} \int dy_1 \cdots dy_N T(y_1, y_2) \cdots T(y_{i-1}, y_i) y_i T(y_i, y_{i+1}) \\
&\quad \cdots T(y_{j-1}, y_j) y_j T(y_j, y_{j+1}) \cdots T(y_N, y_{N+1}) \\
&= \frac{1}{Z_P} \sum_\nu \int dy_i \cdots dy_j \Lambda_\nu^{i-1} \Phi_\nu^L(y_i) y_i T(y_i, y_{i+1}) \\
&\quad \cdots T(y_{j-1}, y_j) y_j \Lambda_\nu^{N-j+1} \Phi_\nu^R(y_j)
\end{aligned}
\tag{3.47}
$$

where the straightforward integrations, i.e the first $i - 1$ and the last $N - j + 1$ have already been performed (cf. above). In order to perform the remaining integrations, we insert two more factors of 1, after y_i and before y_j, i.e. integrals $\int \delta(y_i - \bar{y}_i)$ and $\int \delta(y_j - \bar{y}_j)$, respectively; exploiting the presence of the δ functions, we may substitute the variables y_i and y_j by $\bar{y}_i$ and $\bar{y}_j$ respectively. This translates to two more sums over complete sets of states and another $j - i$ integrals which can now be performed:

$$
\begin{aligned}
< y_i y_j > &= \frac{1}{Z_P} \sum_{\nu,\mu,\rho} \int d\bar{y}_i d\bar{y}_j dy_i \cdots dy_j \Lambda_\nu^{i-1} \Phi_\nu^L(\bar{y}_i) \bar{y}_i \Phi_\mu^R(\bar{y}_i) \Phi_\mu^L(y_i) \\
&\quad T(y_i, y_{i+1}) \cdots T(y_{j-1}, y_j) \Phi_\rho^R(y_j) \Phi_\rho^L(\bar{y}_j) \bar{y}_j \Lambda_\nu^{N-j+1} \Phi_\nu^R(\bar{y}_j) \\
&= \frac{1}{Z_P} \sum_{\nu,\mu,\rho} \Lambda_\nu^{N+i-j} \Lambda_\rho^{j-i} \int d\bar{y}_i d\bar{y}_j \Phi_\nu^L(\bar{y}_i) \bar{y}_i \Phi_\mu^R(\bar{y}_i) \\
&\quad \delta_{\mu,\rho} \Phi_\rho^L(\bar{y}_j) \bar{y}_j \Phi_\nu^R(\bar{y}_j) \\
&= \frac{1}{Z_P} \sum_{\nu,\mu} \Lambda_\nu^{N+i-j} \Lambda_\mu^{j-i} |M_{\nu\mu}|^2 \quad .
\end{aligned}
\tag{3.48}
$$

In the thermodynamic limit the $\nu = 0$ term dominates; the resulting factor cancels against the denominator and leaves

$$
< y_i y_{i+r} > = \sum_\mu |M_{0\mu}|^2 e^{-\beta(\epsilon_\mu - \epsilon_0)r}
\tag{3.49}
$$

where we have used Dirac shorthand for the matrix element and set $j = i + r$. The first term ($\mu = 0$) in the above sum corresponds to $< y >^2$ and should properly be subtracted from both sides; This leaves

$$
\begin{aligned}
< \delta y_i \delta y_{i+r} > &\equiv < y_i y_{i+r} > - < y_i >< y_{i+r} > \\
&= {\sum_\nu}' |M_{0\nu}|^2 e^{-\beta(\epsilon_\nu - \epsilon_0)r}
\end{aligned}
\tag{3.50}
$$

where now the ground state is excluded from the summation. The above result identifies the correlation length ξ, i.e the typical length over which the decay of correlations takes place, as

$$\frac{\xi}{l} = \frac{1}{\beta(\epsilon_1 - \epsilon_0)} \tag{3.51}$$

where the subscript 1 stands for the first excited state (dominant exponential in the limit of large r).

Gradient-expansion approximation to the spectrum of (3.36):

Suppose that the displacement field does not change appreciably over a lattice constant This is certainly reasonable at low temperatures. Note that this does not exclude large displacements per se. Nonlinearity is explicitly allowed, but the displacement field must be smooth. The assumption is certainly reasonable at low temperatures.

We set $y = x + z$, $\Phi^R \to \phi$ and rewrite (3.36) as

$$
\begin{aligned}
e^{-\beta[\epsilon_\nu - V(x)]}\phi_\nu(x) &= \int_{-\infty}^{+\infty} dz\, e^{-\frac{1}{2}\beta\mu\omega_0^2 z^2} \left\{ \phi_\nu(x) + z\phi_\nu'(x) + \frac{1}{2}\phi_\nu''(x) \right\} \\
&= \left[\frac{2\pi}{\beta\mu\omega_0^2}\right]^{1/2} \left\{ \phi_\nu(x) + \frac{1}{2\beta\mu\omega_0^2}\phi_\nu''(x) \right\} \tag{3.52}
\end{aligned}
$$

where higher terms in the gradient expansion have been neglected and the Gaussian integrals have been performed. The factor in front of the r.h.s. can be absorbed in the eigenvalue by defining $\tilde{\epsilon}_\nu = \epsilon_\nu + [1/(2\beta)]\ln[2\pi/(\beta\mu\omega_0^2)]$. Now comes the hard part. For many practical purposes, the relevant size of $\epsilon - V(x)$ is D, the depth of the Morse well (or some other characteristic energy in the case of another potential). In our case one can reasonably argue that this is the case for the lowest eigenstates; at large negative values of x (where this does not hold, because $V(x)$ is huge) we expect that the exact eigenfunction Φ and its approximation ϕ are both negligible, so that the possible large error in computing matrix elements is irrelevant. If then $\beta D \leq 1$ it is reasonable to expand the exponential and keep only the first term. Dividing both sides by β we obtain a Schrödinger - like equation:

$$-\frac{1}{2\mu(\beta\omega_0)^2}\phi_\nu''(x) + [V(x) - \tilde{\epsilon}_\nu]\phi_\nu(x) = 0 \tag{3.53}$$

Before we continue the discussion of (3.53) and its properties, we pick up the bits and pieces (cf (3.32), (3.33), (3.43)) of the thermodynamic free energy (per site)

$$
\begin{aligned}
f &= -\frac{1}{\beta N}\ln(Z_K Z_P) \\
&= -\frac{1}{2\beta}\ln\left(\frac{2\pi\mu}{\beta}\right) + \epsilon_0 \\
&= -\frac{1}{\beta}\ln\left(\frac{2\pi}{\beta\omega_0}\right) + \tilde{\epsilon}_0 \,. \tag{3.54}
\end{aligned}
$$

The first term is the free energy of the small oscillations (transverse phonons in this context). It is a term smooth in temperature (constant specific heat!) and need not concern us any more. No phase transition can come out of it. Any

nontrivial physics is hidden in $\tilde{\epsilon}_0$. It is therefore appropriate to drop the tilde from now on and finally ask the question: what is so special about the ground state of the Morse potential?

I will quote the solution of (3.53) from Landau and Lifshitz; but before I do that, let me make a couple of comments. First, (3.53) would be a true (i.e. quantum-mechanical) Schrödinger equation, if we substituted $1/(\beta\omega_0)$ by $\hbar$. I will come back to that point. Second, I can get a dimensionless potential (and eigenvalue) by dividing both sides of (3.53) by D. In other words, the relevant dimensionless parameter is

$$\delta^2 = \begin{cases} \frac{2\mu}{a^2\hbar^2}\cdot & D \quad \text{(quantum mechanics)} \\[2mm] \frac{2\mu\beta^2\omega_0^2}{a^2}\cdot & D \quad \text{(statistical mechanics).} \end{cases} \tag{3.55}$$

In terms of δ, the bound state spectrum of (3.53) is given by

$$\begin{aligned} \frac{\epsilon_n}{D} &= 1 - \left[1 - \frac{n+1/2}{\delta}\right]^2 \\ n &= 0, 1, ..., int(\delta - 1/2). \end{aligned} \tag{3.56}$$

There is at least one bound state if $\delta > 1/2$. For $1 \geq \delta > 1/2$ there is *exactly* one bound state. And if δ becomes equal to, or smaller than $1/2$, there is no bound state at all. *The value $\delta_c = 1/2$ is "critical".* In quantum mechanical language, if a particle has a mass which is lighter than a critical mass $\mu_c = \hbar^2 a^2/(8D)$, it cannot be confined in the well. Quantum fluctuations will drive it out. (note: this is a general property of 1-dimensional wells which are asymmetric; exercise ... for the half-infinite asymmetric well; symmetric wells will support a particle in a bound state, no matter how low its mass).

In the context of statistical mechanics, δ_c corresponds, via (3.55), to a critical temperature $T_c = 2(\omega_0/a)\sqrt{2\mu D}$. The free energy is given by

$$\frac{f}{D} = \begin{cases} 1 & T > T_c \\[2mm] 1 - \left(1 - \frac{T}{T_c}\right)^2 & T < T_c \ , \end{cases} \tag{3.57}$$

where in the upper line we have made use of the fact that the bottom of the continuum part of the spectrum is at $\epsilon = D$. The free energy f is non-analytic at $T = T_c$, where its second derivative is discontinuous (i.e. there is a jump in the specific heat). This corresponds to a second order transition, according to the Ehrenfest classification scheme[1].

In order to gain some further insight into the physics involved, it is useful to examine the average displacement cf (3.45), determined by the ground-state (GS) eigenfunction

$$\phi_0(x) = e^{-\zeta/2}\, \zeta^{\delta-1/2} \tag{3.58}$$

where $\zeta = 2\delta e^{-ax}$. It is straightforward to see that, as T approaches T_c from below, the eigenfunction extends towards larger and larger positive values of x:

$$\phi_0(x) \propto e^{-\lambda x} \tag{3.59}$$

---

[1] Note that the term "second order" is meant literally in this case, not just as a metaphor for the absence of a latent heat (for which the term "continuous transition" would be appropriate).

where

$$\lambda = \frac{1}{\delta - \delta_c} \tag{3.60}$$

is a (transverse) characteristic length which measures the spatial extent of the GS eigenfunction. As a consequence, we can estimate that $< y >$, which is dominated by the large values of the argument, will also behave as

$$< y > \sim (\delta - \delta_c)^{-1} \sim \left(1 - \frac{T}{T_c}\right)^{-1}. \tag{3.61}$$

[For comparison: the exact result, $< y > = \frac{1}{a}\left[\ln(2\delta) - \psi(2\delta - 1)\right]$ obtained by (3.58), has the asymptotic behavior claimed].

As the critical temperature is approached from below, particles cease to be confined to the minimum of the Morse well. They perform larger and larger excursions to the flatter part of the potential. At T_c the transition is complete; the average transverse displacement is infinite. Particles move, on the average, on the flat top of the Morse potential. Unwinding ("melting") of the DNA has occurred.

In the language of critical phenomena $< y >$ is the order parameter. In the "usual" phase transitions, one goes from an ordered to a disordered phase. The order parameter m vanishes at the transition point, i.e $m \propto (T_c - T)^\beta$ with a positive critical exponent β (not to be confused with the inverse temperature: standard notation of critical phenomena!). DNA melting is really an instability (rather than an "order-disorder" transition). It is therefore not surprising that the corresponding critical exponent β extracted from (3.61) is negative (-1).

Experimental data on DNA denaturation do not deliver $< y >$ directly. The "experimental order parameter" is the helical fraction, i.e the probability that a given base pair is still bound; technically one uses an (instrumentation-dependent) cutoff y_0 and measures $P(y > y_0, T)$. For the model presented here, this function approaches zero smoothly (linearly) as $T \to T_c$, independently of the choice of y_0.

Eq. (3.51) states that the correlation length is also contolled by the gap in the eigenvalue spectrum; as the transition is approached,

$$\frac{\xi}{l} = \frac{1}{\beta D} \left(1 - \frac{T}{T_c}\right)^{-2} \tag{3.62}$$

which identifies a critical exponent $\nu = 2$ for the divergence of the correlation length. The picture of thermal denaturation which emerges is one of ordered regions of typical size ξ, where helical structure persists; these regions are interrupted by "denaturation bubbles".

Comment: The mathematical analogy between the behavior of the spectral gap which occurs in a point (d=0) system and the singularity in the free energy of a classical chain (d=1) is an example of a deeper analogy which relates quantum to thermal fluctuations; the formal correspondence $\hbar \leftrightarrow 1/(\beta\omega_0)$ hides a far-reaching analogy between

$$d - dimensional \ QM \Leftrightarrow (d+1) - dimensional \ classical \ stat. \ mech. \tag{3.63}$$

The analogy is most fruitful at $d = 1$, because of the interplay and the richness of exact available results which based either in the transfer-matrix approach
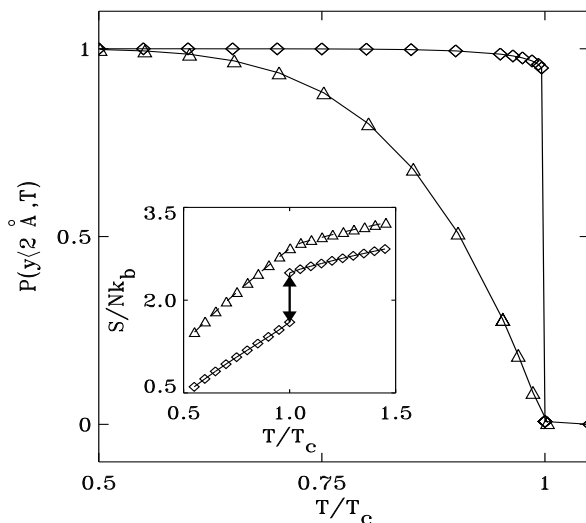
Figure 3.3: The fraction of bound base pairs $P(y < 2\mathring{A}, T)$ as a function of the T/T_c for the type I (triangles) and II (diamonds). Inset: the entropy $S(T)/Nk_B$ (symbols as in main fig.); the length of the double arrow represents the estimate of the melting entropy obtained from the scaling Eq. (3.4). The solid lines are "guides to the eye".

of 2-dimensional classical statistics (Onsager, 2d Ising model) or on the Bethe-Ansatz developed for 1-d quantum spin systems.

The theory presented is by no means complete; in particular it does not seem to account (nor was it proposed for that purpose!) for the series of sharp steps with which melting of physical, heterogeneous DNA occurs. Some of these issues have already been addressed. In particular, in the next lecture I will give a brief account of the mechanism via which a 1st order transition may occur. However, the "morale" of this approach is that it is indeed possible to construct *Hamiltonian* models which exhibit true thermodynamic phase transitions [2].

3.4   Is DNA melting a 1st order transition?

Typical structure revealed in experiments involves a series of steps (multistep melting). Heterogeneity by itself cannot explain that; a distribution of coupling strengths $\{D_i\}$ of the various base pairs gives a smooth transition corresponding to some average $\bar{D}$.

2-chain model, as formulated, misses at least one important feature: the coupling between neighboring base pairs does not seem to depend on the difference coordinate alone. The reason can be seen simply in an extreme case: if either one of the two neighbors belongs to a denaturation bubble, the restoring force

---

[2]There seems to be recent awareness (cf. Hansmann and Okamoto, J. Chem. Phys. **110**, 1267 (1999)) that the $N \to \infty$ limit of the helix-coil transition in polypeptides represents a true phase transition

originating from it cannot be significant. Stiffness is therefore a function of the pair. A simple way to account for this, proposed by Dauxois, Peyrard & Bishop (*Phys. Rev. E* **47**, R44 (1993)), has been to assume that the stiffness constant depends on both displacements as

$$\tilde{\omega}_0^2(y_n, y_{n+1}) = \left[1 + e^{-\alpha(y_n + y_{n+1})}\right]\omega_0^2 \tag{3.64}$$

where α is a characteristic inverse length, typically much smaller than the a of the Morse potential. The above expression "interpolates" between values of $2\omega_0^2$ (when both n and $n+1$ oscillate near the bottom of the well) and ω_0^2 (when either n or $n+1$ reaches the flat top). Note that large *negative* values of the displacement (which might introduce excessive stiffness values) are rendered improbable by the repulsive cores of the Morse potentials at both n and $n+1$.

Introducing this modified stiffness parameter, we obtain, in the spirit of the gradient expansion (3.52),

$$e^{-\beta[\epsilon_\nu - V(x)]}\phi_\nu(x) \quad = \quad \left[\frac{2\pi}{\beta\mu\omega_0^2 f(x)}\right]^{1/2}\left\{\phi_\nu(x) + +\frac{1}{2\beta\mu\omega_0^2 f(x)}\phi_\nu''(x)\right\}$$

where $f(x) = 1 + e^{-2\alpha x}$. The resulting "Schrödinger" equation

$$-\frac{1}{2\mu\beta^2\omega_0^2 f(x)}\phi_\nu''(x) + U(x)\phi_\nu(x) = \tilde{\epsilon}_\nu\phi_\nu(x) \tag{3.65}$$

differs in two aspects from (3.53). First, the "mass" is x-dependent. Second, the potential includes a new term, $U(x) = V(x) + [1/(2\beta)]\ln f(x)$. Fig shows the two contributions to the potential in two typical cases. If $2\alpha/a > 1$, the barrier introduced by f is too weak to control the behavior of U as $x \to \infty$. Alternatively if $2\alpha/a > 1$, the barrier dominates the asymptotic behavior. In the first case, the critical behavior is identical with the one described in the previous section. In the second case it can be shown (either within the WKB approximation to the spectrum of (3.65) or via a high-accuracy numerical solution of the full TI problem) that the gap between the ground state and the bottom of the continuum now approaches zero *linearly*:

$$\epsilon_1 - \epsilon_0 = AD\left(1 - \frac{T}{T_c}\right) \tag{3.66}$$

where A is a numerical factor of order unity. This implies a correlation length which diverges with an exponent $\nu = 1$ and a discontinuity in the first derivative of the free energy, i.e. a melting entropy

$$\Delta s = -\lim_{T \to T_c^-}\frac{\partial f}{\partial T} = \frac{AD}{T_c} \tag{3.67}$$

corresponding to a latent heat $\Delta H_{melting} = AD$. The transition is first order.

In order to explore the critical properties of the phase transition, it is convenient to introduce an additional term

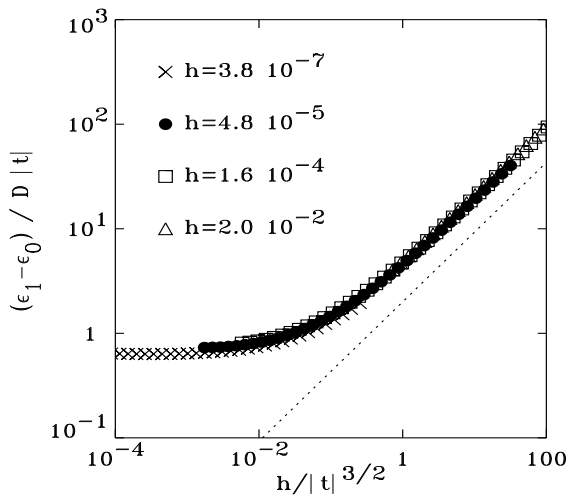$$H_1(y) = Dah\sum_n y_n \tag{3.68}$$

44

Figure 3.4: The dependence of $(\epsilon_1 - \epsilon_0)/D|t|$ on the scaling variable $h/|t|^{3/2}$ is shown for 4 different values of h and a range of temperatures; the dotted line marks the slope 2/3.

in the transverse Hamiltonian. The conjugate field h has the property that it "confines" particles to finite values of the displacement field; one can therefore study the transition in the limit $h \to 0^+$.

Numerical results suggest (cf. Fig. (3.4)) that

$$\epsilon_1 - \epsilon_0 = D|t|\Psi\left(\frac{h}{|t|^{3/2}}\right) \tag{3.69}$$

where $t = T/T_c - 1$. Since this is (minus) the singular part of the free energy, differentiation with respect to h gives the order parameter

$$< y > \propto |t|^{-1/2} \tag{3.70}$$

i.e. the exponent $\beta = -1/2$. Note that there is no step in the order parameter, which diverges continuously as approaches the critical point. There is however a step discontinuity in the *observed* "order parameter", i.e. the fraction of bound pairs (see Fig. (3.3)).

We have derived in this section a "melting scenario" for a hypothetical, homogeneous, DNA of infinite length. "Real life" DNA is expected to present this behavior only as an approximation. Multistep melting due to heterogeneity has already been shown to occur (Cule & Hwa, *PRL* **79**, 2375 (1997)) in the context of this model. There is significant variety in the possibilities of critical behavior of simple 1-d models.

3.5 Phase transitions in one-dimensional systems

Consider the following statements:

1. complete myth: *there are no phase transitions in one dimensional systems.*

2. half-truth (trickier!): *There are no phase transitions in 1-d systems with short-range interactions.*

3. true statement (van Hove, 1950): *No phase transitions occur in 1-d particle systems with short-range* **pair** *interactions.*
   Model just described has on-site potential - i.e. this statement is not applicable.

4. However, Landau has an even stronger statement!
   Macroscopic phase coexistence [and therefore a phase transition] cannot occur at finite temperatures in one dimensional systems.

Derivation: Consider a system with N sites, which may exist in either phase A or phase B. Let θ be the fraction of phase A; furthermore, let there be $m << N$ contacts between the phases, each of energy ϵ. These can be steplike (Ising) or continuous domain walls. The free energy of the configuration is given by

$$F = N\theta f_A + N(1-\theta)f_B + F_{DW} \tag{3.71}$$

where

$$F_{DW} = m\epsilon - k_B T S_{DW}(m, N) \tag{3.72}$$

and the (dimensionless) entropy is given by

$$S_{DW}(m, N) = \ln[\frac{N!}{m!(N-m)!}] \tag{3.73}$$

$$\approx m\ln[\frac{Ne}{m}]$$

Minimization of the total free energy with respect to m yields

$$0 = \frac{\partial F}{\partial m} = \epsilon + k_B T \ln(\frac{m}{N}) \tag{3.74}$$

and a macroscopic average number (ie. a *finite density*) of domain walls

$$\bar{m} = Ne^{-\epsilon/(k_B T)} . \tag{3.75}$$

The system breaks up into m regions of finite size $e^{\epsilon/(k_B T)}$. Macroscopic phase separation can only occur at zero temperature (as the domain size goes to infinity).

Summary of Landau's argument in words:
No phase transition can take place in 1-d, because the system splits into a macroscopic (of order N) number of domains of finite size, separated by domain walls. The spontaneous split is favored by entropy, which more than makes up for the energy needed to create the domain walls.

Landau's argument covers a wide range of systems, e.g. double-well on-site potentials ("Ising" universality class). Is there a way out? Yes, since the argument is based on a finite domain wall energy. If that energy for some reason diverges, the argument does not apply and phase separation can take place.

(cf. exercise 5, evaluate DW energy for ϕ^4 and Morse on-site potentials)

Chapter 4

Stochastic resonance phenomena

4.1 General background: escape from a barrier

Kramers' problem: Activate Barrier Crossing (ABC); Basis of all chemistry (reaction rates) - microscopic derivation of Arrhenius law.

Physical modelling (Kramers): particle in metastable potential $V(x)$ with a minimum at $x = 0$ and a local maximum at $x = a$ with a characteristic energy difference $\Delta E = V(a) - V(0)$ (cf. Fig. 4.1).

Also present: thermal noise and a viscous medium.

Wanted: the escape rate $\tau(\Delta E)$; Arrhenius limit $\tau(\Delta E) \propto e^{\Delta E/(k_B T)}$.

Equation of motion

$$m\dot{v} + m\gamma v = -V'(x) + f(t) \quad \text{(Langevin)} \tag{4.1}$$

where the random force satisfies

$$< f(t) > \quad = \quad 0 \tag{4.2}$$
$$< f(t)f(t') > \quad = \quad A\delta(t - t') \tag{4.3}$$

(short time correlations, approximated by a δ function: "white noise"). Note that A is not arbitrary. Its value is fixed by the system parameters as follows: Consider the "stochastic" part of the velocity and displacements, respectively :

$$m\Delta v(t) = \int_0^t dt' e^{-\gamma(t-t')} f(t') \tag{4.4}$$

and

$$\Delta x(t) = \int_0^t dt' \Delta v(t') \,. \tag{4.5}$$

Eq. (4.4) is equivalent to (4.1) for the case of a vanishing deterministic force $F = -V'(x)$. It is straightforward to show (exercise ...) that

$$< \Delta v^2(t) >= \frac{A}{2\gamma m^2} \left(1 - e^{-2\gamma t}\right) \,. \tag{4.6}$$
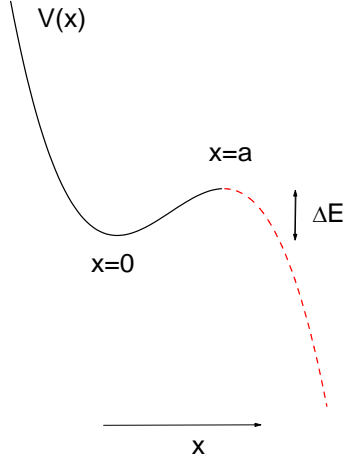
47

Figure 4.1: Schematic form of the potential in the one-dimensional Kramers problem. The unstable portion is shown as a dashed curve.

In the limit $t \rightarrow \infty$ the demand of energy equipartition requires the r.h.s to approach $k_B T/m$. Therefore

$$A = 2\gamma m k_B T \quad (fluctuation\text{-}dissipation). \tag{4.7}$$

Furthermore, one can show that, in the limit $\gamma t >> 1$,

$$< \Delta x^2(t) >= 2Dt \tag{4.8}$$

where

$$D = \frac{A}{2m^2\gamma^2} = \mu k_B T \quad (Einstein\ relation), \tag{4.9}$$

and $\mu = (m\gamma)^{-1}$ is the mobility of the particle. Mobility in the (standard) following sense: if we take the overdamped limit of Eq. (4.1), where the inertial term vanishes, then, on the average,

$$m\gamma < v >= F \tag{4.10}$$

i.e. $v_{drift} = \mu F$ (mobility: proportionality constant relating drift velocity and force when a particle moves under the influence of a constant force in a viscous medium).

There are two alternative descriptions of random phenomena. One involves stochastic differential equations (Langevin). The other is in terms of continuous probability distributions. Outline the second:

Let $P(x,t)dx$ be the probability to find a particle in the interval $(x, x + dx)$ at time t. The function P, being a probability density, obeys an equation of

48

continuity, i.e.

$$\frac{\partial}{\partial t}P(x,t) + \frac{\partial}{\partial x}J(x,t) = 0 \tag{4.11}$$

where the probability current has, in general, a drift and a diffusion term:

$$
\begin{aligned}
J(x,t) &= P(x,t)v_{drift} - D\frac{\partial P}{\partial x} \\
&= -P\mu V'(x) - \mu k_B T\frac{\partial P}{\partial x} \tag{4.12}
\end{aligned}
$$

Inserting (4.12) in (4.11) and dividing both sides by μ, we obtain

$$\frac{1}{\mu}\frac{\partial}{\partial t}P(x,t) = \frac{\partial}{\partial x}[V'(x)P] + k_B T\frac{\partial^2 P}{\partial x^2} \tag{4.13}$$

It is usual to redefine the units of temperature and time by setting $k_B = 1$ and $\mu = 1$. Eq. (4.13) is known as the *Smoluchowski* equation. Note: the "derivation" presented here is not a substitute for a good course in the theory of random variables. But it can hopefully give you a feeling for some of the physical concepts which lie behind the formalism.

The following formal way of rewriting (4.13) in terms of a linear operator will prove useful:

$$\frac{\partial P}{\partial t} = T\frac{\partial}{\partial x}e^{-V(x)/T}\frac{\partial}{\partial x}e^{V(x)/T}P \equiv \mathcal{L}P \tag{4.14}$$

Defining $P = e^{-V(x)/(2T)}\tilde{P}$ gives

$$e^{-V(x)/(2T)}\dot{\tilde{P}} = e^{-V(x)/(2T)}\left\{ T\tilde{P}'' - \underbrace{\left[\frac{V'(x)^2}{4T} - \frac{1}{2}V''(x)\right]}_{U(x)}\tilde{P} \right\}, \tag{4.15}$$

or,

$$\dot{\tilde{P}} = -\mathcal{H}\tilde{P} \tag{4.16}$$

in terms of the pseudoSchrödinger operator

$$\mathcal{H} = -T\frac{\partial^2}{\partial x^2} + U(x). \tag{4.17}$$

A separation of variables *Ansatz*

$$\tilde{P}(x,t) = \sum_j A_j\,\phi_j(x)\,e^{-\lambda_j t} \tag{4.18}$$

leads to the eigenvalue equation

$$\mathcal{H}\phi_j(x) = \lambda_j\phi_j(x). \tag{4.19}$$

The problem is therefore reduced to finding the eigenfunctions and eigenvalues of $\mathcal{H}$, subject to the appropriate initial and boundary conditions.

If the particle is initially at $x = 0$

$$
\begin{aligned}
P(x, 0) &= \delta(x - x_0) \\
&= e^{-\frac{V(x) - V(x_0)}{2T}} \sum_j \phi_j^*(x_0) \phi_j(x) \tag{4.20}
\end{aligned}
$$

where the second line exploits the completeness of the eigenfunctions; the prefactor is unity if $x = x_0$ and irrelevant otherwise. Comparing (4.20) to (4.18) provides the constants A_j. The resulting formal solution of the initial value problem is

$$
P(x|x_0, t) = e^{-\frac{V(x) - V(x_0)}{2T}} \sum_j \phi_j^*(x_0) \phi_j(x) e^{-\lambda_j t} . \tag{4.21}
$$

Some general remarks on (4.21):
Eq. (4.13) has a special, time-independent, exact solution of the form

$$
P_\infty = \frac{1}{Z} e^{-V(x)/T} \tag{4.22}
$$

where $Z = \int dx \, \exp[-V(x)/T]$, from the normalization of probability. This is not necessarily a stable equilibrium solution. It *may* be, depending on the boundary conditions of the problem.

The eigenvalue equation (4.19) has the formal solution

$$
\phi_0(x) = \frac{1}{\sqrt{Z}} e^{-V(x)/(2T)} \tag{4.23}
$$

associated with the eigenvalue $\lambda = 0$. Although this is always a formal solution, i.e. independently of the form of the potential $V(x)$, note that there may exist situations where it does not represent an admissible eigenfunction. This happens when the normalization integral Z does not exist; the Kramers problem is one such case!

The spectrum of (4.19) is nonnegative:

$$
\lambda_j \geq 0 \quad all \, j \tag{4.24}
$$

Corollary: *If Z exists, then*

$$
\lim_{t \to \infty} P(x|x_0, t) = P_\infty \tag{4.25}
$$

We now proceed to treat the Kramers problem:
For a non-steady-state situation, a probability leak at $x = a$ (absorbing trap) and a reflecting barrier at $x = b$, and an initial condition of the form (4.20) with $b < x_0 < a$ (particle starting off within the barrier), the relevant quantity is

$$
I(t) = \int_b^a dx \, P(x|x_0, t) \tag{4.26}
$$

and expresses the probability that the particle is still confined within the barrier at time t. Note the general properties

$$
\begin{aligned}
\dot{I}(t) &< 0 \tag{4.27} \\
I(0) &= 1 \tag{4.28} \\
I(\infty) &= 0 . \tag{4.29}
\end{aligned}
$$

Let $f(t)\delta t$ be the probability that an escape takes place in the time interval $(t, t + \delta t)$. The relationship

$$I(t) = I(t + \delta t) + f(t)\delta t \qquad (4.30)$$

reflects the fact that, there are only two possible outcomes at $t + \delta t$ and their probabilities are additive. It follows that

$$f(t) = -\dot{I}(t) . \qquad (4.31)$$

The average first passage time is given as

$$
\begin{aligned}
\tau_1(x_0) &\equiv \int_0^\infty dt\, f(t)\, t \qquad &(4.32)\\
&= -\int_0^\infty dt\, \dot{I}(t) = -tI(t)|_0^\infty + \int_0^\infty dt\, I(t)\\
&= \int_0^\infty dt \int_b^a dx\, P(x|x_0, t) \qquad &(4.33)\\
&= \int_a^b dx\, e^{-\frac{V(x)-V(x_0)}{2T}} \underbrace{\sum_j \frac{\phi_j^*(x_0)\phi_j(x)}{\lambda_j}}_{\equiv M(x,x_0)} . \qquad &(4.34)
\end{aligned}
$$

A "zeroth order" approximation suggests that if $0 < \lambda_0 << \lambda_1 < \lambda_2 < \cdots$, the $j = 0$ term dominates the last sum (slow leak); introducing

$$\phi_0(x) \approx \frac{1}{\sqrt{Z}} e^{-V(x)/(2T)} \qquad (4.35)$$

as an *approximate* eigenfunction in (4.34), we obtain

$$\tau_1 \approx \frac{1}{\lambda_0} \qquad (4.36)$$

as an order-of-magnitude estimate. of the average first passage time. We can and will do better than that, but it is reassuring to know that if a characteristic (slow) time scale exists, in the form of a well separated ground-state eigenvalue, it will show up in the barrier escape phenomenon as well.

Exact evaluation of τ_1: note first that the kernel $M(x, x_0)$ defined in (4.34) satisfies

$$\mathcal{L}(x)M(x, x_0) = -\delta(x - x_0) \qquad (4.37)$$

(can be verified explicitly). A formal solution of (4.37) is

$$M(x, x_0) = \frac{1}{T} e^{-V(x)/T} \int_x^a dy\, e^{V(y)/T} \int_b^y dz\, \delta(z - x_0) . \qquad (4.38)$$

We then obtain from (4.34)

$$
\begin{aligned}
\tau_1(x_0) &= \frac{1}{T} \int_b^a dx\, e^{-V(x)/T} \int_x^a dy\, e^{V(y)/T} \int_b^y dz\, \delta(z - x_0)\\
&= \frac{1}{T} \int_{x_0}^a dx\, e^{V(x)/T} \int_b^x dy\, e^{-V(y)/T} \qquad (4.39)
\end{aligned}
$$

which is our general result for the mean first-passage time in terms of the potential.

Application to a wedge-type potential with a trap at $x = a$ and $x_0 = 0$:

$$V(x) = \begin{cases} Ex/a & \text{if } 0 < x < a \\ \\ \infty & \text{if } x < 0 \end{cases} \tag{4.40}$$

(analytically tractable, just to demonstrate how Arrhenius temperature dependence comes about). From (4.39) we obtain

$$\begin{aligned} \tau_1(0) &= \frac{1}{T} \int_0^a dx\, e^{Ex/(Ta)} \int_0^x dy\, e^{-Ey/(Ta)} \\ &= \frac{a^2 T}{E} \left\{ e^{E/T} - 1 - \frac{T}{E} \right\} . \end{aligned} \tag{4.41}$$

In particular, we obtain the limiting cases

$$\tau_1(0) = \begin{cases} \frac{a^2 T}{E^2}\, e^{E/T} & \text{if } T << E \ (Arrhenius) \\ \\ \frac{a^2}{2T} & \text{if } T >> E \end{cases} \tag{4.42}$$

4.2 Escape from fluctuating barriers

4.3 Fluctuation-driven ratchets

References: Asturian & Bier *PRL* **72**, 1766 (1994); Bier, *Contemp. Phys.* **38**, 381 (1997).

Rudimentary model of a molecular motor:

(i) *microtubule*: essentially an array of dipoles, forming a saw-tooth like potential (asymmetric with respect to reflection).

(ii) *motor protein* (kinesin) moving along the microtubule.

As the electrically charged motor protein moves, it catalyzes ATP hydrolysis. Depending on the phase of the catalysis cycle, it may or may not be bound to the ATP molecule. In the first case its electrical charge becomes neutralized, in the second it persists. Accordingly it ignores or feels the electrostatic potential of the microtubule, which can be viewed as a "fluctuating ratchet". In what follows, the motor protein is approximated by a Brownian particle.

Model (Fig).

$$V_0(x) = \begin{cases} E_0 \frac{\xi}{al} & \text{if } 0 < \xi < al \\ \\ E_0 \frac{l-\xi}{(1-a)l} & \text{if } al < \xi < l \end{cases} \tag{4.43}$$

where l is the periodicity of the microtubule array, $1 > a > 1/2$ its asymmetry, E_0 the maximum of the potential, and $\xi = x\, mod\, l$. The potential fluctuates according to the pattern

$$V(x, t) = \begin{cases} V_0(x) & \text{if } t/(2\tau)\, mod\, 1 < 1/2 \\ \\ 0 & \text{if } t/(2\tau)\, mod\, 1 > 1/2 \end{cases} \tag{4.44}$$

(*dichotomous noise*: the potential is turned on and off at time intervals of duration τ).

It is now possible to solve the Smoluchowski equation (4.13), which describes the motion of an overdamped particle in the above time-dependent potential. However.if the barrier is high, i.e. $E_0 >> k_B T$, the salient physics of transport is contained in the following argument:

Every time the barrier goes up, it confines the particle to one of the potential minima. The deterministic force acting on it, as it attempts to climb the barrier, dominates and sents it back. The particle stays at the minimum for time τ. When the barrier is turned off, the particle has a chance to diffuse. During the time interval τ it can travel over a mean diffusion distance $\sqrt{2D_0 T}$. (The subscript 0 denotes that this is the diffusion constant of the medium; the presence of the fluctuating ratchet will modify the diffusional behavior of the particle; this is what we are attempting to estimate!).

Suppose that the time τ is so short, that the typical diffusion distance is much smaller than the lattice constant l. At first glance, nothing will happen. The barrier will go up again and the particle will be trapped again. Let's look closer: is it cetrain that it will be trapped *at the same site?*.

This is where the asymmetry comes in. If a is substantially larger than $1/2$, the time may be too short for the particle to diffuse over a full lattice constant, or over the long side of the saw-tooth. But it may be enough for it to diffuse leftward, over the short-side [length $(1-a)l$] of the saw-tooth (remember: the barrier is off). In this case, when the barrier comes up again, the particle will find itself on the top, slide downhill to the neighboring (left) site and get trapped there. If the process can be statistically repeated, we have a steady current.

In formal language:

Starting with a particle at the position $x = 0$ at time $t = 0$, $P(x,0) = \delta(x)$. Diffusion equation (NB: (4.13) without the potential term) over time τ gives a probability evolution

$$P(x,\tau) = \frac{1}{2\sqrt{\pi D_0 \tau}} \, e^{-\frac{x^2}{4D_0 \tau}} \; . \tag{4.45}$$

Probability that the particle moves a notch to the right

$$\begin{aligned} \pi_R &= \int_{al}^{\infty} dx \, P(x,\tau) \\ &= \frac{1}{\sqrt{\pi}} \int_{\frac{al}{2\sqrt{D_0\tau}}}^{\infty} dy \, e^{-y^2} \\ &= \frac{1}{2} erfc\left(\frac{al}{2\sqrt{D_0\tau}}\right) \; . \tag{4.46} \end{aligned}$$

Probability that the particle moves a notch to the left (similarly):

$$\begin{aligned} \pi_L &= \int_{-\infty}^{(a-1)l} dx \, P(x,\tau) \\ &= \frac{1}{2} erfc\left(\frac{(1-a)l}{2\sqrt{D_0\tau}}\right) \; . \tag{4.47} \end{aligned}$$

Probability that the particle stays in same groove because it does not diffuse far enough in either direction: $1 - \pi_L - \pi_R$

We can now write down a master equation, describing the particle's motion through the sites (labeled by integers). If $P_m(t)$ be the probability that the particle is at the $m - th$ site at time t,

$$P_m(t + 2\tau) = P_m(t)\{1 - \pi_L - \pi_R\} + P_{m+1}(t)\pi_L + P_{m-1}(t)\pi_R \qquad (4.48)$$

the three terms on the r.h.s. of (4.48) express the probabilities of the three possible outcomes as outlined above. Multiplying (4.48) by ml and summing over all m, we obtain

$$\bar{x}(t + 2\tau) = \bar{x}(t) + (\pi_R - \pi_L)l \qquad (4.49)$$

where

$$\bar{x}(t) = l \sum_m P_m(t)m \qquad (4.50)$$

is the mean displacement of the particle at time t. The resulting drift velocity (particle flux) is

$$\bar{v} = \frac{\pi_R - \pi_L}{2\tau} l \ . \qquad (4.51)$$

Similarly, multiplying both sides of (4.48) by $l^2 m^2$ and summing over all m, we obtain

$$\overline{x^2}(t + 2\tau) = \overline{x^2}(t) - (\pi_R - \pi_L)^2 l^2 + (\pi_R + \pi_L) l^2 \qquad (4.52)$$

where

$$\overline{x^2}(t) = l^2 \sum_m P_m(t)m^2 \ . \qquad (4.53)$$

Subtracting $\bar{x}^2(t + 2\tau)$ from both sides of (4.52), we obtain

$$\overline{x^2}(t + 2\tau) - \bar{x}^2(t + 2\tau) = \overline{x^2}(t) - \bar{x}^2(t) + (\pi_R + \pi_L) l^2 - (\pi_R - \pi_L)^2 l^2 \ . \qquad (4.54)$$

Identifying

$$\overline{x^2}(t) - \bar{x}^2(t) = 2 D t \qquad (4.55)$$

yields

$$D = \frac{\pi_R + \pi_L - (\pi_R - \pi_L)^2}{2\tau} l^2 \ . \qquad (4.56)$$

Comment: formalism describes a general asymmetric random walk. Extreme special cases are (i) $\pi_R = \pi_L$ (symmetic, no drift, nonzero diffusion constant), (ii) $\pi_R = 0$, $\pi_L = 1$ (full "drift", no diffusion; in fact, deterministic motion except for "waiting phase" when the potential is on and the particle remains trapped).

In the spirit of our approximation (cf. above), assume that the probability of "left-drifting" is small but nonnegligible, whereas that of right-drifting is negligible; accordingly, we use the asymptotic expansion

$$erfc(x) \sim \frac{1}{\sqrt{\pi}x} e^{-x^2} \ (x >> 1) \ , \qquad (4.57)$$

and obtain a flux

$$
\begin{aligned}
J(\tau) = \bar{v} \quad &\approx \quad -\frac{\pi_L l}{2\tau} \\
&\approx \quad -\frac{1}{2(1-a)} \sqrt{\frac{D_0}{\pi\tau}} e^{-\frac{(1-a)^2 l^2}{4 D_0 \tau}} \ .
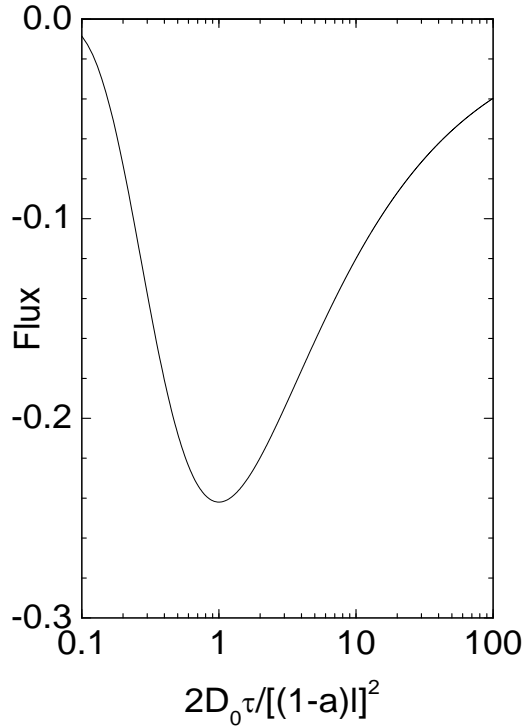\end{aligned}
\qquad (4.58)
$$

Figure 4.2: The dependence of the flux on the flipping rate; note the logarithmic scale. The magnitude of the flux has a maximum when the flipping rate is such that the particle, on average, has the time to diffuse over the nearest (i.e. the left) side of the barrier.

As a function of τ, the flux has a maximum at

$$\tau_R = \frac{(1-a)^2 l^2}{2D_0} \ . \tag{4.59}$$

This is exactly the time it takes for the particle to diffuse over a mean characteristic distance $(1-a)l$, i.e. to diffuse "over the top of the (absent) barrier". Tuning the flipping rate $1/\tau$ (which is in reality a non-white noisy process) to the diffusion rate of Brownian motion is known as *stochastic resonance*. The flux (4.58) is shown in Fig. (4.2). At its maximum, the flux has the value

$$J_R = -(2\pi e)^{-1/2} \frac{l}{2\tau_R} \tag{4.60}$$

i.e., the particle moves at the rate of a constant fraction of sites per flip of the barrier. This can be viewed as a measure of the efficiency of the stochastic resonance mechanism.

Note that in this discussion we have made no mention of the energy source of the whole process, which is of course the hydrolysis of ATP. The emphasis

was on describing the statistical mechanics of a simple case of the stochastic resonance phenomenon.